

## SLOWLY ROTATING RELATIVISTIC STARS. II. MODELS FOR NEUTRON STARS AND SUPERMASSIVE STARS

JAMES B. HARTLE\*

University of California, Santa Barbara

AND

KIP S. THORNE†

California Institute of Technology, Pasadena

*Received January 12, 1968*

### ABSTRACT

The equilibrium configurations of rigidly rotating white dwarfs and neutron stars are calculated using the Harrison-Wheeler and the Tsuruta-Cameron  $V_\gamma$  equations of state, along with the general-relativistic equations of structure. The equations of structure used are the exact relativistic equations with one exception: they have been expanded in powers of the angular velocity  $\Omega$ , and terms of higher order than  $\Omega^2$  have been neglected. The equilibrium configurations of slowly rotating supermassive stars are also calculated.

### I. INTRODUCTION

The recent discoveries of galactic X-ray sources and quasi-stellar radio sources, together with progress in the dynamical theory of supernovae, has led to a renewal of interest in the general-relativistic theory of stellar structure. This subject had its beginnings in the 1939 analysis of Oppenheimer and Volkoff of a non-rotating star made from an ideal neutron gas. More recently, a number of authors have calculated in greater detail the relativistic equilibrium configurations of cold white dwarfs, neutron stars, and supermassive stars, when these stars are not rotating. (For reviews of these calculations see Harrison *et al.* 1965; Thorne 1967; and Wheeler 1967.)

It is now appropriate to abandon the restriction that relativistic stellar models be non-rotating and to investigate the effects of angular velocity on the structure of relativistic stars. In this series of papers we examine the case of stars which rotate rigidly and slowly. In Paper I (Hartle 1967) the equations of structure for slowly rotating relativistic stars were derived. Terms of greater than second order in the angular velocity were neglected in these equations, but no other approximations were made. In this paper (Paper II) these equations are integrated numerically for particular equations of state corresponding to white-dwarf matter, neutron-star matter, and supermassive-star matter. The stability of the equilibrium configurations calculated here, and the gravitational waves which they emit when perturbed, will be discussed in subsequent papers of this series.

In § II the equations of structure are summarized; in § III they are applied to the calculation of white-dwarf and neutron-star models; and in § IV they are used to calculate models for supermassive stars. Some properties of the exterior gravitational fields of slowly rotating stars are examined in the Appendix.

### II. EQUATIONS OF STRUCTURE

The method used to construct models for rigidly and slowly rotating relativistic stars is summarized briefly here. For details and derivations the reader should refer to Paper I, the notation of which we follow.

\* Supported in part by the National Science Foundation.

† Alfred P. Sloan Research Fellow and John Simon Guggenheim Fellow. Work supported in part by the National Science Foundation (GP-7976) (formerly (GP-5391)) and by the Office of Naval Research (Nonr-220(47)).

a) *An Equation of State Is Assumed*

As the first step in the calculation of a slowly rotating stellar model, a one-parameter equation of state,

$$E = E(P) , \quad N = N(P) , \quad (1)$$

is specified. Here  $P$  is the pressure,  $E$  is the total density of mass-energy, and  $N$  is the number density of baryons. For neutron stars and white dwarfs this relation will be one of the equations of state for cold degenerate matter, while for supermassive stars, it will be the polytropic equation of state of index 3.

b) *Values for the Central Density and Angular Velocity Are Chosen*

For slow rotation, once the equation of state is specified, there is a unique equilibrium configuration for each choice of the central density and angular velocity. The small perturbations away from a non-rotating equilibrium configuration are all proportional to the angular velocity or to its square. Consequently, for a given central density, all the models of different angular velocities can be obtained from a single model by scaling. In this paper the results are given in tabular and graphical form for the angular velocity  $\Omega$  satisfying<sup>1</sup>

$$\Omega^2 = M/R^3 , \quad (2)$$

where  $M$  is the mass of the non-rotating configuration and  $R$  is its radius.<sup>2</sup> This is approximately the critical angular velocity at which rotational shedding will occur, and it is thus an upper bound on those angular velocities for which the assumption of slow rotation could be valid.

Having chosen a value of the angular velocity for each value of the central density, one constructs a sequence of equilibrium models by integrating the general-relativistic equations of structure for a sequence of central densities. The integration procedure is the following.

c) *A Non-rotating Stellar Model Is Computed*

For a given value of the central density, the non-rotating equilibrium configuration is determined by integrating the Tolman-Oppenheimer-Volkoff equation of hydrostatic equilibrium for the pressure,  $P(r)$ , and the mass interior to a given radius,  $M(r)$ :

$$\frac{dP}{dr} = -(E + P) \frac{(M + 4\pi r^3 P)}{r(r - 2M)} , \quad (3a)$$

$$dM/dr = 4\pi r^2 E . \quad (3b)$$

The integration is performed outward, starting at the star's center,  $r = 0$ . At the star's center  $M$  is 0;  $E$  is the given central density,  $E_c$ ; and  $P$  is  $P(E_c)$  as given by the equation of state (eq. [1]). The radius of the surface of the star,  $R$ , is that value of  $r$  at which  $P(r)$  drops to zero; and the value of  $M(r)$  there is the star's total mass.

The metric that describes the spherically symmetric geometry of the non-rotating star has the Schwarzschild form

$$ds^2 = -e^{\nu(r)} dt^2 + [1 - 2M(r)/r]^{-1} dr^2 + r^2(d\theta^2 + \sin^2 \theta d\phi^2) . \quad (3c)$$

The remaining function in the metric,  $\nu(r)$ , is determined by integrating outward from the center the equation

$$d\nu/dr = -2(E + P)^{-1}(dP/dr) \quad (3d)$$

with the boundary condition  $\nu(\infty) = 0$ .

<sup>1</sup> Here, and throughout, we use units in which  $c = G = 1$ .

<sup>2</sup> In this paper the radius of the non-rotating star will be denoted by  $R$  rather than by  $a$ , as it was in Paper I.

The total number of baryons in the non-rotating star can be found from the integral

$$A = \int_0^R N(r)[1 - 2M(r)/r]^{-1/2} 4\pi r^2 dr . \quad (3e)$$

For further discussion of the construction of non-rotating stellar models see Thorne (1967).

*d) The Rotational Perturbations in the Metric and Stress-Energy Tensor Are Specified*

When the equilibrium configuration described above is set into slow rotation, the geometry of spacetime around it and its interior distribution of stress-energy are changed. With an appropriate choice of coordinates, the perturbed geometry is described by

$$ds^2 = -e^\nu[1 + 2(h_0 + h_2P_2)]dt^2 + \frac{[1 + 2(m_0 + m_2P_2)/(r - 2M)]}{1 - 2M/r} dr^2 \quad (4)$$

$$+ r^2[1 + 2(v_2 - h_2)P_2][d\theta^2 + \sin^2 \theta(d\phi - \omega dt)^2] + O(\Omega^3) .$$

Here,  $P_2 = P_2(\cos \theta) = (3 \cos^2 \theta - 1)/2$  is the Legendre polynomial of order 2;  $\omega$ , which we call "the angular velocity of the local inertial frame,"<sup>3</sup> is a function of  $r$  and is proportional to the star's angular velocity  $\Omega$ ; and  $h_0, h_2, m_0, m_2, v_2$  are all functions of  $r$  that are proportional to  $\Omega^2$ .

In the above coordinate system the fluid inside the star moves with the 4-velocity appropriate to uniform and rigid rotation (see, e.g., Thorne 1967, p. 332), of which the contravariant components are

$$u^t = (-g_{tt} - 2\Omega g_{t\phi} - g_{\phi\phi}\Omega^2)^{-1/2}$$

$$= e^{-\nu/2}[1 + \frac{1}{2}r^2 \sin^2 \theta(\Omega - \omega)^2 e^{-\nu} - h_0 - h_2P_2] , \quad (5)$$

$$u^\phi = \Omega u^t , \quad u^r = u^\theta = 0 .$$

The quantity

$$\bar{\omega} \equiv \Omega - \omega , \quad (6)$$

which appears in the expression for  $u^t$ , is the angular velocity of the fluid relative to the local inertial frame. It plays a fundamental role in the equations of structure below.

The baryon number density, the density of mass-energy, and the pressure of the fluid are affected by the rotation because the rotation deforms the star. In the interior of the star at given  $(r, \theta)$ , in a reference frame that is momentarily moving with the fluid, the pressure is

$$P + (E + P)(p_0^* + p_2^*P_2) \equiv P + \Delta P ; \quad (7a)$$

the density of mass-energy is

$$E + (E + P)(dE/dP)(p_0^* + p_2^*P_2) \equiv E + \Delta E ; \quad (7b)$$

and the number density of baryons is

$$N + (E + P)(dN/dP)(p_0^* + p_2^*P_2) \equiv N + \Delta N . \quad (7c)$$

Here,  $p_0^*$  and  $p_2^*$  are dimensionless functions of  $r$ , proportional to  $\Omega^2$ , which describe the pressure perturbation; all other parameters were defined above. The stress-energy tensor for the fluid in the rotating star is, of course,

$$T_\mu^\nu = -(E + \Delta E + P + \Delta P)u_\mu u^\nu + (P + \Delta P)\delta_\mu^\nu . \quad (8)$$

<sup>3</sup> Note that these "local inertial frames" are *not* the frames in which Coriolis forces are absent. The Coriolis-free frames are discussed in Landau and Lifschitz (1962, p. 362). Cf. Hartle (1967) for further discussion.

The rotational perturbations of the star's structure are described by the functions  $\bar{\omega}$ ,  $h_0$ ,  $m_0$ ,  $p_0^*$ ,  $h_2$ ,  $m_2$ ,  $v_2$ ,  $p_2^*$ . These functions are calculated from Einstein's field equations as described below.

*e) The "Rate of Rotation of an Inertial Frame" and the Moment of Inertia Are Determined*

In equilibrium, a rotating star attains a balance between pressure forces, gravitational forces, and centrifugal forces. The magnitude of the centrifugal force is determined not by the angular velocity  $\Omega$  of the fluid relative to a distant observer but by its angular velocity relative to the local inertial frame,  $\bar{\omega}(r)$ . This quantity is of first order in  $\Omega$  and is found by integrating the differential equation

$$\frac{1}{r^4} \frac{d}{dr} \left( r^4 j \frac{d\bar{\omega}}{dr} \right) + \frac{4}{r} \frac{dj}{dr} \bar{\omega} = 0, \quad (9)$$

where

$$j(r) = e^{-\nu(r)/2} [1 - 2M(r)/r]^{1/2}. \quad (10)$$

The solution must be regular at the origin; and outside the star it takes the form

$$\bar{\omega}(r) = \Omega - 2J/r^3, \quad (11)$$

where  $J$  is the total angular momentum of the star. The moment of inertia of the star is defined as the ratio  $J/\Omega$  and is conveniently expressed in terms of the radius of gyration,  $R_g$ :

$$R_g = (\text{moment of inertia}/M)^{1/2} = (J/\Omega M)^{1/2}. \quad (12)$$

In practice, one integrates equation (9) outward from the center of the star, where the boundary conditions  $\bar{\omega} = \bar{\omega}_c$  and  $d\bar{\omega}/dr = 0$  are imposed. The constant  $\bar{\omega}_c$  is chosen arbitrarily. When one reaches the surface—and only then—one can determine the angular velocity,  $\Omega$ , and angular momentum,  $J$ , corresponding to  $\bar{\omega}_c$ :

$$J = \frac{1}{6} R^4 \left( \frac{d\bar{\omega}}{dr} \right)_{r=R}, \quad \Omega = \bar{\omega}(R) + \frac{2J}{R^3} \quad (13)$$

(cf. eq. [11]). If a different value of  $\Omega$  is desired, one rescales the function  $\bar{\omega}(r)$  to obtain it:

$$\bar{\omega}(r)_{\text{new}} = \bar{\omega}(r)_{\text{old}} (\Omega_{\text{new}}/\Omega_{\text{old}}). \quad (14)$$

*f) The Spherical Deformations of the Star Are Calculated*

The spherical part of the rotational deformation is calculated by integrating the  $l = 0$  equations of hydrostatic equilibrium for the "mass perturbation factor"  $m_0$  and the "pressure perturbation factor"  $p_0^*$ :<sup>4</sup>

$$\frac{dm_0}{dr} = 4\pi r^2 \frac{dE}{dP} (E + P) p_0^* + \frac{1}{12} j^2 r^4 \left( \frac{d\bar{\omega}}{dr} \right)^2 - \frac{1}{3} r^3 \frac{dj^2}{dr} \bar{\omega}^2, \quad (15a)$$

$$\begin{aligned} \frac{dp_0^*}{dr} = & - \frac{m_0(1 + 8\pi r^2 P)}{(r - 2M)^2} - \frac{4\pi(E + P)r^2}{(r - 2M)} p_0^* + \frac{1}{12} \frac{r^4 j^2}{(r - 2M)} \left( \frac{d\bar{\omega}}{dr} \right)^2 \\ & + \frac{1}{3} \frac{d}{dr} \left( \frac{r^3 j^2 \bar{\omega}^2}{r - 2M} \right). \end{aligned} \quad (15b)$$

These equations are integrated outward, with the boundary conditions that both  $m_0$  and  $p_0^*$  vanish at the origin. With these boundary conditions, the rotating star will have the

<sup>4</sup> These equations were written in Paper I in terms of the variable  $R$  introduced there; but in the limit of slow rotation the equations are the same when written in terms of  $r$  as when written in terms of  $R$ .

same central density as the non-rotating one (cf. eq. [7b]). Outside the star,  $m_0$ , which is one of the perturbations in the metric tensor, is given by

$$m_0 = \delta M - J^2/r^3, \quad (15c)$$

where  $\delta M$  is a constant. Consequently, the total mass-energy of the star with central density  $E_c$  and angular velocity  $\Omega$  is

$$M(R) + \delta M = M(R) + m_0(R) + J^2/R^3, \quad (16)$$

where  $R$  is the radius of the star's surface.

Once  $p_0^*$ ,  $\delta M$ , and  $J$  have been calculated, one obtains the function  $h_0(r)$  from the algebraic relations

$$h_0 = -\frac{\delta M}{r - 2M} + \frac{J^2}{r^3(r - 2M)} \quad \text{outside the star,} \quad (17a)$$

$$h_0 = -p_0^* + \frac{1}{3}r^2e^{-\nu}\bar{\omega}^2 + h_{0c}, \quad \text{inside the star.} \quad (17b)$$

Here  $h_{0c}$  is a constant determined by the demand that  $h_0$  be continuous across the star's surface.

The binding energy of a relativistic star is the difference between its rest mass and its total mass-energy:

$$E_B = \mu A - M. \quad (18)$$

Here the rest mass has been expressed as the product of the total baryon number,  $A$ , and the rest mass per baryon,  $\mu$ . The change in binding energy,  $\delta E_B$ , of the rotating over the non-rotating star is calculated from  $m_0$ ,  $p_0^*$ , and the density of internal energy,

$$\epsilon = E - \mu N, \quad (19)$$

through the formulae

$$\begin{aligned} \delta E_B &= -\frac{J^2}{R^3} + \int_0^R 4\pi r^2 B(r) dr, \\ B(r) &= (E + P)p_0^* \left\{ \frac{dE}{dP} \left[ \left(1 - \frac{2M}{r}\right)^{-1/2} - 1 \right] - \frac{d\epsilon}{dP} \left(1 - \frac{2M}{r}\right)^{-1/2} \right\} \\ &\quad + (E - \epsilon) \left(1 - \frac{2M}{r}\right)^{-3/2} \left[ \frac{m_0}{r} + \frac{1}{3}j^2r^2\bar{\omega}^2 \right] \\ &\quad - \frac{1}{4\pi r^2} \left[ \frac{1}{12}j^2r^4 \left(\frac{d\bar{\omega}}{dr}\right)^2 - \frac{1}{3} \frac{dj^2}{dr} r^3\bar{\omega}^2 \right]. \end{aligned} \quad (20)$$

The change in the total baryon number is then obtained from equation (18).

#### g) The Quadrupole Deformations of the Star Are Calculated

One calculates the quadrupole part of the deformations by integrating the  $l = 2$  equations

$$\frac{dv_2}{dr} = -\frac{dv}{dr} h_2 + \left(\frac{1}{r} + \frac{1}{2} \frac{dv}{dr}\right) \left[ -\frac{1}{3}r^3 \frac{dj^2}{dr} \bar{\omega}^2 + \frac{1}{6}j^2r^4 \left(\frac{d\bar{\omega}}{dr}\right)^2 \right], \quad (21a)$$

$$\begin{aligned} \frac{dh_2}{dr} &= \left\{ -\frac{dv}{dr} + \frac{r}{r - 2M} \left(\frac{dv}{dr}\right)^{-1} \left[ 8\pi(E + P) - \frac{4M}{r^3} \right] \right\} h_2 \\ &\quad - \frac{4v_2}{r(r - 2M)} \left(\frac{dv}{dr}\right)^{-1} + \frac{1}{6} \left[ \frac{1}{2} \frac{dv}{dr} r - \frac{1}{r - 2M} \left(\frac{dv}{dr}\right)^{-1} \right] r^3 j^2 \left(\frac{d\bar{\omega}}{dr}\right)^2 \\ &\quad - \frac{1}{3} \left[ \frac{1}{2} \frac{dv}{dr} r + \frac{1}{r - 2M} \left(\frac{dv}{dr}\right)^{-1} \right] r^2 \frac{dj^2}{dr} \bar{\omega}^2, \end{aligned} \quad (21b)$$

subject to the four boundary conditions

$$h_2 = v_2 = 0 \quad \text{at} \quad r = 0 \quad \text{and at} \quad r = \infty . \quad (21c)$$

Outside the star  $h_2$  and  $v_2$  have the analytic form

$$h_2 = J^2 \left( \frac{1}{Mr^3} + \frac{1}{r^4} \right) + KQ_2^2 \left( \frac{r}{M} - 1 \right) , \quad (22a)$$

$$v_2 = -\frac{J^2}{r^4} + K \frac{2M}{[r(r-2M)]^{1/2}} Q_2^1 \left( \frac{r}{M} - 1 \right) , \quad (22b)$$

where  $K$  is a constant and  $Q_n^m$  is the associated Legendre polynomial of the second kind.

Once  $h_2$  and  $v_2$  have been calculated from equations (21), the non-radial mass and pressure perturbation factors,  $m_2$  and  $p_2^*$ , are determined from the algebraic relations

$$m_2 = (r - 2M) \left[ -h_2 - \frac{1}{3}r^3(dj^2/dr)\bar{\omega}^2 + \frac{1}{6}r^4j^2(d\bar{\omega}/dr)^2 \right] , \quad (23a)$$

$$p_2^* = -h_2 - \frac{1}{3}r^2e^{-\nu}\bar{\omega}^2 . \quad (23b)$$

The rotational deformation of the star is most clearly understood as follows: The surface of constant given density that lies at radius  $r$  in the non-rotating configuration is displaced in the rotating configuration to radius

$$r + \xi_0(r) + \xi_2(r)P_2(\cos \theta) , \quad (24a)$$

where

$$\xi_0 \equiv \delta r = -p_0^*(E + P)/(dP/dr) , \quad \xi_2 = -p_2^*(E + P)/(dP/dr) . \quad (24b)$$

Equation (24a) describes the surfaces of constant density in a particular coordinate system. An invariant parameterization of a surface of constant density can be obtained by embedding it in a three-dimensional flat space. To do this, we ask for the surface in a three-dimensional flat space with polar coordinates  $r^*$ ,  $\theta^*$ ,  $\phi^*$ , which has the same intrinsic geometry as the surface of constant density in our star. Accurate to order  $\Omega^2$ , the desired 3-surface in flat space is the spheroid

$$r^*(\theta^*) = r + \xi_0(r) + \{\xi_2(r) + r[v_2(r) - h_2(r)]\}P_2(\cos \theta^*) . \quad (25a)$$

The mean radius of this spheroid is

$$\bar{r}^* = r + \xi_0(r) , \quad (25b)$$

and its eccentricity is

$$\begin{aligned} e &= [(\text{radius at equator})^2/(\text{radius at pole})^2 - 1]^{1/2} \\ &= [-3(v_2 - h_2 + \xi_2/r)]^{1/2} . \end{aligned} \quad (25c)$$

The mean radius of the star and the eccentricity of its surface we denote by  $\bar{R} = R + \delta R$  and  $e_s$ , respectively; and we calculate them by setting  $r = R$  in equations (25).

The deformation of the star's external gravitational field is determined by the metric perturbation factors  $h_2$ ,  $v_2$ , and  $m_2$  of equations (22) and (23). Far from the star,  $h_2$  becomes the non-radial perturbation in the Newtonian potential and thereby determines the star's quadrupole moment to be

$$Q \equiv [\text{coefficient of } r^{-3}P_2(\cos \theta) \text{ term in Newtonian potential}] = \frac{8}{5}KM^3 + J^2/M . \quad (26)$$

Here  $K$  is the constant in equations (22), which is determined by the numerical integration of equations (21).<sup>5</sup>

Some of the properties of the exterior gravitational field of a slowly rotating star are examined in the Appendix; and a more careful definition of the quadrupole moment than equation (26) is also given there.

<sup>5</sup> The factor  $\frac{1}{6}$  quoted in eq (138) of paper I is in error

## III. WHITE-DWARF AND NEUTRON-STAR MODELS

a) *Equations of State*

Slowly rotating white-dwarf and neutron-star models are presented here for two equations of state: (1) the Harrison-Wheeler (HW) equation of state (see Harrison *et al.* 1965, chap. viii) and (2) the  $V_\gamma$  equation of state proposed by Tsuruta and Cameron (1966), with the form  $P = E$  imposed above  $1.08 \times 10^{16} \text{ g cm}^{-3}$ . Harrison and Wheeler idealize matter at high densities as an equilibrium mixture of non-interacting, degenerate nucleons and electrons. The equilibrium is established through the weak interactions of the constituents, but all strong interactions are neglected. This idealization is probably inaccurate at densities much above  $10^{13} \text{ g cm}^{-3}$  and is certainly inaccurate above nuclear densities ( $4 \times 10^{14} \text{ g cm}^{-3}$ ). In the  $V_\gamma$  equation of state, the equilibrium mixture is enlarged to include some of the hyperons, and a phenomenological baryon-baryon potential is included to approximate the effects of the strong interactions. However, so few of the properties of matter in bulk at near-nuclear densities and above have been calculated accurately that either equation of state will give only a qualitative description of stars with central densities in this region.

In our computations the HW and  $V_\gamma$  equations of state were used in tabular form, with logarithmic interpolation between table entries. The HW table used is given in Table 1. This version of the HW equation of state, which was obtained from B. K. Harrison (private communication), has been used in all previous computations of Harrison-Wakano-Wheeler (HWW) stellar models (Harrison *et al.* 1965; Meltzer and Thorne 1966). However, it differs slightly from the more accurate version given on page 109 of Harrison *et al.* Our version of the  $V_\gamma$  equation of state is given in Table 2. It was condensed and adapted from a more extensive table, kindly given to us by S. Tsuruta and A. G. W. Cameron. In both equations of state, the internal energy density,  $\epsilon$ , was calculated from the equation of state  $E = E(P)$  by integrating the equation of adiabatic compression,

$$\frac{dN}{N} \equiv \frac{d(E - \epsilon)}{E - \epsilon} = \frac{dE}{E + P}. \quad (27)$$

b) *Structure of Non-rotating Stars*

The non-rotating equilibrium configurations of matter obeying the HW equation of state have been calculated previously and discussed in detail by Harrison, Wakano, and Wheeler (1958). (See also Harrison *et al.* 1965; Meltzer and Thorne 1966; Thorne 1967.) The properties of these non-rotating "HWW configurations," as recalculated in connection with the present investigation, are summarized in Table 3 (masses, radii, etc., for thirty models) and in Figure 6 (internal distributions of density and pressure for four representative models). In Table 3 the two distinct families of stable configurations—white dwarfs at  $E_c < 2.5 \times 10^8 \text{ g cm}^{-3}$ , and neutron stars at  $5.0 \times 10^{13} < E_c < 6.0 \times 10^{15} \text{ g cm}^{-3}$ —are delineated clearly.

The non-rotating  $V_\gamma$  configurations have been calculated previously and discussed by Tsuruta and Cameron (1966). Their properties, as recalculated in connection with the present investigation, are summarized in Table 4 and Figure 10. Again the division into white dwarfs, neutron stars, and unstable stars is clear.

c) *Effects of Rotation on the Stellar Structure*

The effects of rotation on the structures of the HWW and the  $V_\gamma$  configurations have been calculated using the procedure outlined in § II. The results of those calculations are presented in Table 5 and Figures 1, 3, and 5–9 for the HWW configurations, and in Table 6 and Figures 2, 4, 5, and 10–13 for the  $V_\gamma$  configurations. Detailed discussions of the results are contained in the table footnotes, in the figure captions, and in the text below.

TABLE 1  
HARRISON-WHEELER EQUATION OF STATE\*

P	E	$\epsilon$	P	E	$\epsilon$
8.31E-41	5.82E-28	1.00E-45	2.73E-21	2.34E-18	9.21E-21
4.17E-40	5.84E-28	7.11E-43	6.49E-21	4.68E-18	2.25E-20
8.31E-40	5.86E-28	2.77E-42	1.10E-20	7.41E-18	4.05E-20
4.17E-39	5.97E-28	4.16E-41	1.86E-20	1.17E-17	7.21E-20
8.31E-39	6.04E-28	1.12E-40	3.05E-20	1.86E-17	1.28E-19
2.79E-38	6.32E-28	8.64E-40	4.58E-20	2.95E-17	2.25E-19
2.38E-37	8.52E-28	3.36E-38	6.59E-20	4.68E-17	3.88E-19
1.37E-36	1.23E-27	3.21E-37	9.55E-20	7.41E-17	6.60E-19
7.00E-36	2.34E-27	3.47E-36	1.50E-19	1.17E-16	1.11E-18
6.96E-35	6.54E-27	5.01E-35	2.54E-19	1.86E-16	1.88E-18
4.79E-34	1.56E-26	3.76E-34	4.49E-19	2.95E-16	3.17E-18
1.74E-33	2.95E-26	1.52E-33	9.14E-19	4.68E-16	5.39E-18
5.95E-33	5.22E-26	5.18E-33	1.88E-18	7.41E-16	9.28E-19
1.56E-32	8.52E-26	1.45E-32	6.09E-18	1.48E-15	2.18E-17
4.62E-32	1.53E-25	4.73E-32	2.63E-17	3.71E-15	7.27E-17
2.67E-31	3.71E-25	2.72E-31	8.23E-17	7.41E-15	1.90E-16
9.63E-31	7.41E-25	1.05E-30	2.60E-16	1.48E-14	5.16E-16
4.83E-30	1.86E-24	5.82E-30	1.09E-15	3.71E-14	2.02E-15
2.32E-29	4.68E-24	3.03E-29	3.25E-15	7.41E-14	5.70E-15
5.19E-29	7.41E-24	6.82E-29	9.71E-15	1.48E-13	1.61E-14
1.65E-28	1.48E-23	2.27E-28	3.93E-14	3.71E-13	6.30E-14
8.23E-28	3.71E-23	1.11E-27	9.71E-14	7.41E-13	1.69E-13
2.37E-27	7.41E-23	3.59E-27	2.42E-13	1.48E-12	4.34E-13
7.19E-27	1.48E-22	1.12E-26	7.34E-13	3.71E-12	1.43E-12
2.69E-26	3.71E-22	4.84E-26	1.65E-12	7.41E-12	3.37E-12
7.86E-26	7.41E-22	1.42E-25	3.60E-12	1.48E-11	7.71E-12
1.93E-25	1.48E-21	4.03E-25	1.01E-11	3.71E-11	2.23E-11
6.60E-25	3.71E-21	1.53E-24	2.08E-11	7.41E-11	4.87E-11
1.65E-24	7.41E-21	4.07E-24	4.28E-11	1.48E-10	1.04E-10
4.18E-24	1.48E-20	1.07E-23	1.10E-10	3.71E-10	2.82E-10
1.35E-23	3.71E-20	3.77E-23	2.26E-10	7.41E-10	5.89E-10
3.29E-23	7.41E-20	9.57E-23	4.64E-10	1.48E-09	1.22E-09
8.07E-23	1.48E-19	2.41E-22	1.19E-09	3.71E-09	3.19E-09
2.67E-22	3.71E-19	8.17E-22	2.43E-09	7.41E-09	6.52E-09
6.53E-22	7.41E-19	2.04E-21	4.91E-09	1.48E-08	1.33E-08
1.21E-21	1.17E-18	3.72E-21	1.23E-08	3.71E-08	3.41E-08

\* This version of the HW equation of state, which was kindly given to us by B. Kent Harrison, differs slightly from that presented on p. 109 of Harrison, Thorne, Wakano, and Wheeler (1965). Here  $P$ , the pressure,  $E$ , the total density of mass-energy, and  $\epsilon = E - \mu N$ , the density of internal energy, are all measured in  $\text{cm}^{-2}$ . To convert to  $\text{g cm}^{-3}$ , divide by  $Gc^2 = 0.742 \times 10^{-28}$   $\text{cm g}^{-2}$ . In this table and all others, computer notation is used: .742E - 28 stands for  $0.742 \times 10^{-28}$ . For densities above  $3.71 \times 10^{-8}$  the equation of state is given analytically by

$$P = E/3 \quad \epsilon = E - 0.30 \times 10^{-8} (E/3.71 \times 10^{-8})^{3/4}.$$

TABLE 2  
 $V_\gamma$  EQUATION OF STATE\*

P	E	$\epsilon$	P	E	$\epsilon$
4.9836E-39	7.7697E-30	7.4750E-39	5.0797E-20	5.9361E-17	4.7476E-19
4.9836E-29	7.7697E-24	7.4750E-29	6.0582E-20	7.4766E-17	6.1217E-19
1.0036E-28	1.1760E-23	1.4929E-28	7.5031E-20	9.4146E-17	7.8808E-19
2.1205E-28	1.8638E-23	3.2137E-28	9.6859E-20	1.1855E-16	1.0142E-18
4.1366E-28	2.8210E-23	6.3769E-28	1.6060E-19	1.8793E-16	1.6790E-18
9.2884E-28	4.6817E-23	1.4638E-27	2.1986E-19	2.3670E-16	2.1628E-18
1.9215E-27	7.4200E-23	3.0959E-27	3.0559E-19	2.9806E-16	2.7896E-18
3.9377E-27	1.1760E-22	6.5039E-27	4.2968E-19	3.7532E-16	3.6053E-18
7.9880E-27	1.8638E-22	1.3563E-26	6.0693E-19	4.7261E-16	4.6703E-18
1.6023E-26	2.9540E-22	2.8063E-26	8.5554E-19	5.9526E-16	6.0666E-18
3.1794E-26	4.6828E-22	5.7589E-26	1.1982E-18	7.4956E-16	7.8976E-18
6.2408E-26	7.4217E-22	1.1711E-25	1.6786E-18	9.4407E-16	1.0309E-17
1.2127E-25	1.1763E-21	2.3606E-25	2.3391E-18	1.1891E-15	1.3491E-17
2.3348E-25	1.8642E-21	4.7164E-25	3.2632E-18	1.4976E-15	1.7696E-17
4.4601E-25	2.9546E-21	9.3455E-25	4.5808E-18	1.8863E-15	2.3275E-17
8.4614E-25	4.6839E-21	1.8377E-24	6.4720E-18	2.3763E-15	3.0709E-17
1.5960E-24	7.4234E-21	3.5858E-24	9.2075E-18	2.9937E-15	4.0656E-17
2.9967E-24	1.1768E-20	6.9517E-24	1.3275E-17	3.7714E-15	5.4033E-17
5.6058E-24	1.8651E-20	1.3391E-23	1.9255E-17	4.7523E-15	7.2157E-17
1.0458E-23	2.9567E-20	2.5664E-23	2.5896E-17	5.6716E-15	9.0343E-17
1.9215E-23	4.6860E-20	4.8876E-23	4.0657E-17	7.3435E-15	1.2631E-16
3.4178E-23	7.4285E-20	9.2308E-23	6.4245E-17	9.3176E-15	1.7366E-16
6.0721E-23	1.1776E-19	1.7268E-22	1.0201E-16	1.1639E-14	2.3654E-16
1.0776E-22	1.8668E-19	3.2051E-22	1.8148E-16	1.5080E-14	3.4545E-16
1.9114E-22	2.9594E-19	5.9105E-22	2.8777E-16	1.8315E-14	4.6678E-16
3.3880E-22	4.6914E-19	1.0840E-21	5.1457E-16	2.3046E-14	6.8244E-16
6.0040E-22	7.4371E-19	1.9788E-21	1.2344E-15	3.1132E-14	1.1864E-15
1.0635E-21	1.1790E-18	3.5983E-21	2.3908E-15	3.9756E-14	1.9504E-15
1.8834E-21	1.8690E-18	6.5205E-21	4.3086E-15	5.0327E-14	3.2214E-15
3.3353E-21	2.9635E-18	1.1785E-20	6.2081E-15	6.5706E-14	5.7296E-15
5.9039E-21	4.6990E-18	2.1244E-20	1.5168E-14	8.5389E-14	1.0057E-14
1.0453E-20	7.4508E-18	3.8210E-20	2.5777E-14	1.0877E-13	1.6690E-14
1.8503E-20	1.1814E-17	6.8590E-20	4.9050E-14	1.4812E-13	3.0933E-14
3.6706E-20	2.0545E-17	1.3811E-19	8.1234E-14	1.9121E-13	5.0115E-14
3.7484E-20	2.2522E-17	1.5494E-19	1.6078E-13	2.7804E-13	9.6820E-14
3.8180E-20	2.7059E-17	1.9370E-19	2.9400E-13	4.0032E-13	1.7434E-13
3.9097E-20	3.1053E-17	2.2793E-19	5.3314E-13	5.9320E-13	3.1244E-13
4.0977E-20	3.7317E-17	2.8190E-19	7.1030E-13	7.2628E-13	4.1459E-13
4.5086E-20	4.7142E-17	3.6730E-19	8.0000E-13	8.0000E-13	4.7278E-13

\* Adapted from a more extensive table which was kindly given to us by Sachiko Tsuruta and A. G. W. Cameron. The notation is the same as in Table 1. At low densities ( $E \lesssim 10^{-24}$ ) the equation of state is that of a polytrope of index 1.5:

$$P \propto E^{5/3}, \quad \epsilon \propto P.$$

At densities above those in the table, the equation of state is given analytically by

$$P = \bar{E}, \quad \epsilon = E - 3.2722 \times 10^{-13} (E/8.0000 \times 10^{-13})^{1/2}.$$

TABLE 3  
NONROTATING H-W-W CONFIGURATIONS\*

$E_c$ , g/cm <sup>3</sup>	R, km	$M/M_\odot$	$E_B/M_\odot$ †	$z_s$	$z_c$	Stable?
1.00E03	1.77E4	3.95E-3	6.72E-10	3.30E-7	6.30E-7	yes
1.00E04	1.73E4	3.10E-2	4.04E-08	2.64E-6	5.35E-6	yes
1.00E05	1.44E4	1.33E-1	8.47E-07	1.36E-5	2.99E-5	yes
1.00E06	1.08E4	4.58E-1	1.28E-05	6.25E-5	1.43E-4	yes
1.00E07	7.24E3	9.41E-1	7.09E-05	1.92E-4	4.90E-4	yes
1.00E08	4.66E3	1.17E+0	1.30E-04	3.70E-4	1.15E-3	yes
2.50E08	3.75E3	1.19E+0	1.37E-04	4.67E-4	1.56E-3	yes
1.00E09	2.70E3	1.15E+0	1.17E-04	6.27E-4	2.38E-3	no
1.00E10	1.43E3	1.01E+0	1.40E-05	1.05E-3	4.71E-3	no
1.00E11	7.93E2	8.50E-1	-2.07E-04	1.58E-3	8.62E-3	no
1.00E12	6.87E2	6.71E-1	-4.94E-04	1.44E-3	1.18E-2	no
1.00E13	1.43E3	5.59E-1	-6.14E-04	5.78E-4	1.59E-2	no
1.50E13	2.31E3	4.83E-1	-6.49E-04	3.09E-4	1.77E-2	no
1.70E13	2.78E3	4.25E-1	-6.65E-04	2.25E-4	1.84E-2	no
2.00E13	2.41E3	2.62E-1	-6.95E-04	1.61E-4	1.94E-2	no
2.50E13	4.28E2	1.78E-1	-7.15E-04	6.13E-4	2.15E-2	no
5.00E13	6.91E1	2.05E-1	-6.36E-04	4.39E-3	3.19E-2	yes
1.00E14	3.60E1	2.66E-1	-1.66E-04	1.10E-2	4.93E-2	yes
3.00E14	2.08E1	4.05E-1	2.62E-03	2.99E-2	9.95E-2	yes
1.00E15	1.42E1	5.54E-1	9.40E-03	6.30E-2	2.03E-1	yes
3.00E15	1.02E1	6.61E-1	1.86E-02	1.12E-1	3.88E-1	yes
6.00E15	8.41E0	6.84E-1	2.16E-02	1.47E-1	5.66E-1	yes
1.00E16	7.48E0	6.68E-1	1.93E-02	1.65E-1	7.10E-1	no
3.00E16	5.96E0	5.77E-1	3.44E-03	1.83E-1	1.10E+0	no
1.00E17	5.15E0	4.62E-1	-1.68E-02	1.66E-1	1.62E+0	no
3.00E17	5.18E0	3.87E-1	-2.84E-02	1.33E-1	2.23E+0	no
1.00E18	6.01E0	3.62E-1	-3.14E-02	1.03E-1	3.15E+0	no
3.00E18	6.69E0	3.92E-1	-2.85E-02	9.92E-2	4.33E+0	no
1.00E19	6.72E0	4.27E-1	-2.49E-02	1.09E-1	6.17E+0	no
1.00E20	6.28E0	4.27E-1	-2.48E-02	1.19E-1	1.18E+1	no

\* The various columns are as follows:  $E_c$ , central density of total mass-energy; R, radius  $\equiv$  (surface area of star/ $4\pi$ )<sup>1/2</sup>;  $M/M_\odot$ , total mass-energy of star as measured gravitationally by a distant observer, in units of solar masses;  $E_B/M_\odot$ , binding energy in solar-mass units (defined by eq [18] with  $\mu$  taken as the mass of one <sup>56</sup>Fe atom);  $z_s$ , gravitational redshift,  $\Delta\lambda/\lambda$ , of a photon emitted from the star's surface and received at infinity;  $z_c$ , gravitational redshift of a neutrino emitted from the star's center and received at infinity; "Stable?", an entry "yes" means the star is stable against all *radial* perturbations; "no" means it is unstable against some radial perturbations (cf. Thorne 1967, § 7.5.1). The entries in this and subsequent tables are all accurate to about 1 per cent or better.

† These binding energies are somewhat different from those quoted by Harrison *et al.* (1965). The earlier ones are in error. Notice that there are stable neutron stars with negative binding energies in the range  $2.5E13 < E_c < 1.0E14$  (This was originally discovered by B. K. Harrison and J. A. Wheeler (private communication)).

TABLE 4  
NONROTATING  $V_\gamma$  CONFIGURATIONS\*

$E_c, \text{ g/cm}^3$	R, km	$M/M_\odot$	$E_B/M_\odot$	$z_s$	$z_c$	Stable?
1.00E04	2.20E4	3.70E-2	3.95E-8	2.47E-6	5.84E-6	yes
1.00E05	1.50E4	1.17E-1	5.79E-7	1.15E-5	2.71E-5	yes
1.00E06	1.02E4	3.34E-1	6.76E-6	4.82E-5	1.16E-4	yes
1.00E07	6.65E3	6.86E-1	4.02E-5	1.52E-4	3.94E-4	yes
1.00E08	4.08E3	1.00E+0	1.16E-4	3.62E-4	1.06E-3	yes
1.00E09	2.37E3	1.15E+0	1.88E-4	7.14E-4	2.42E-3	yes
1.00E10	1.43E3	9.94E-1	4.87E-5	1.03E-3	4.51E-3	no
1.00E11	8.13E2	7.52E-1	-2.38E-4	1.36E-3	7.94E-3	no
1.00E12	6.42E2	6.45E-1	-3.93E-4	1.48E-3	1.06E-2	no
4.73E12	8.50E2	6.28E-1	-4.19E-4	1.09E-3	1.19E-2	no
1.00E13	1.10E3	6.39E-1	-4.09E-4	8.55E-4	1.31E-2	no
4.50E13	2.41E3	7.60E-1	-3.32E-4	4.65E-4	1.79E-2	no
5.70E13	3.17E3	7.13E-1	-3.50E-4	3.32E-4	1.92E-2	no
7.18E13	5.17E3	3.02E-1	-4.24E-4	8.60E-5	2.05E-2	no
7.80E13	7.91E2	9.99E-2	-4.38E-4	1.86E-4	2.12E-2	no
8.41E13	2.94E2	9.69E-2	-4.39E-4	4.86E-4	2.22E-2	no
1.00E14	1.02E2	1.01E-1	-4.35E-4	1.46E-3	2.48E-2	yes
2.40E14	1.79E1	2.02E-1	5.20E-4	1.71E-2	5.91E-2	yes
5.00E14	1.27E1	6.48E-1	2.30E-2	8.48E-2	1.97E-1	yes
1.00E15	1.20E1	1.40E+0	1.39E-1	2.34E-1	5.74E-1	yes
1.70E15	1.11E1	1.82E+0	2.66E-1	3.93E-1	1.16E+0	yes
3.00E15	9.87E0	1.95E+0	3.25E-1	5.50E-1	2.25E+0	yes
5.00E15	8.91E0	1.89E+0	2.87E-1	6.32E-1	3.73E+0	no
1.00E16	8.00E0	1.72E+0	1.80E-1	6.55E-1	6.69E+0	no
3.00E16	7.49E0	1.55E+0	1.42E-2	5.98E-1	1.20E+1	no
1.00E17	7.47E0	1.45E+0	-9.39E-2	5.27E-1	2.16E+1	no
3.00E17	7.69E0	1.45E+0	-7.84E-2	5.00E-1	3.75E+1	no
1.00E18	7.81E0	1.49E+0	-4.66E-2	5.08E-1	6.96E+1	no
1.00E19	7.78E0	1.50E+0	-3.58E-2	5.24E-1	2.25E+2	no
1.00E20	7.75E0	1.50E+0	-4.31E-2	5.22E-1	7.12E+2	no

\* The notation is the same as that in Table 3

TABLE 5  
SLOWLY ROTATING H-W-W CONFIGURATIONS\*

$E_c, \text{ g/cm}^3$	$R_g/R$	$\Omega, \text{ sec}^{-1}$	$\omega_s/\Omega$	$\omega_c/\Omega$	$\delta R/R$	$\delta M/M$	$\delta E_B/M_\odot$	$e_s$	$Q/(MR^2)$
—	—	$\propto \Omega$	—	—	$\propto \Omega^2$	$\propto \Omega^2$	$\propto \Omega^2$	$\propto \Omega$	$\propto \Omega^2$
1.00E03	0.526	9.75E-3			0.209	0.498	2.85E-10	1.27	2.00E-1
1.00E04	.508	2.81E-2	1.4 E-6	5.7 E-6	.202	.449	2.53E-08	1.23	1.68E-1
1.00E05	.479	7.66E-2	6.34E-6	3.81E-5	.196	.376	4.76E-07	1.17	1.26E-1
1.00E06	.463	2.20E-1	2.68E-5	1.90E-4	.195	.339	6.67E-06	1.15	1.07E-1
1.00E07	.430	5.73E-1	7.08E-5	6.51E-4	.198	.271	3.22E-05	1.11	7.59E-2
1.00E08	.379	1.24E+0	1.06E-4	1.53E-3	.212	.191	5.18E-05	1.06	4.33E-2
2.50E08	.357	1.73E+0	1.19E-4	2.08E-3	.219	.162	5.48E-05	1.05	3.34E-2
1.00E09	.327	2.79E+0	1.34E-4	3.16E-3	.230	.127	5.34E-05	1.03	2.28E-2
1.00E10	.283	6.81E+0	1.68E-4	6.24E-3	.246	.0853	4.85E-05	1.02	1.22E-2
1.00E11	.248	1.50E+1	1.94E-4	1.14E-2	.260	.0597	3.98E-05	1.01	6.93E-3
1.00E12	.211	1.65E+1	1.28E-4	1.55E-2	.279	.0430	2.02E-05	1.01	4.30E-3
1.00E13	.195	5.05E+0	4.38E-5	2.08E-2	.291	.0446	8.40E-06	1.01	4.84E-3
1.50E13	.208	2.28E+0	2.66E-5	2.31E-2	.292	.0594	5.66E-06	1.01	7.51E-3
1.70E13	.211	1.62E+0	2.00E-5	2.40E-2	.293	.0654	4.15E-06	1.01	8.54E-3
2.00E13	.162	1.58E+0	8.38E-6	2.53E-2	.310	.0405	1.17E-06	1.01	4.99E-3
2.50E13	.0733	1.73E+1	6.57E-6	2.79E-2	.326	.00541	3.03E-07	1.00	4.49E-4
5.00E13	.160	2.87E+2	2.23E-4	4.09E-2	.292	.0144	1.63E-06	1.00	7.01E-4
1.00E14	.255	8.67E+2	1.41E-3	6.20E-2	.246	.0522	5.93E-05	1.01	4.91E-3
3.00E14	.355	2.43E+3	7.19E-3	1.18E-1	.201	.128	8.02E-04	1.03	2.18E-2
1.00E15	.404	5.07E+3	1.88E-2	2.17E-1	.181	.163	2.95E-03	1.04	3.35E-2
3.00E15	.433	9.10E+3	3.59E-2	3.50E-1	.163	.162	5.41E-03	1.03	3.50E-2
6.00E15	.444	1.23E+4	4.73E-2	4.43E-1	.154	.149	5.70E-03	1.02	3.22E-2
1.00E16	.444	1.45E+4	5.20E-2	5.03E-1	.152	.137	4.98E-03	1.01	2.91E-2
3.00E16	.425	1.90E+4	5.16E-2	6.16E-1	.161	.107	2.55E-03	0.99	2.10E-2
1.00E17	.380	2.12E+4	3.81E-2	7.11E-1	.188	.0818	1.16E-03	0.99	1.35E-2
3.00E17	.334	1.92E+4	2.45E-2	7.78E-1	.217	.0701	9.22E-04	0.99	9.92E-3
1.00E18	.309	1.49E+4	1.70E-2	8.39E-1	.233	.0723	1.00E-03	1.00	9.46E-3
3.00E18	.323	1.32E+4	1.80E-2	8.83E-1	.227	.0840	1.33E-03	1.00	1.14E-2
1.00E19	.341	1.37E+4	2.18E-2	9.20E-1	.216	.0902	1.65E-03	1.00	1.30E-2
1.00E20	0.344	1.51E+4	2.37E-2	9.62E-1	0.213	0.0862	1.56E-03	1.00	1.25E-2

\* All quantities in this table are given for the uniform angular velocity  $\Omega = (M/R^3)^{1/2}$ , which is roughly the angular velocity at which equatorial shedding occurs (very rapid rotation!). The properties of more slowly rotating configurations are obtained by scaling the entries in this table in the manner indicated beneath each column heading. The various columns are as follows:  $E_c$ , central density of total mass-energy;  $R_g/R$ , radius of gyration (eq. [12]) in units of stellar radii;  $\Omega$ , angular velocity of star as measured by a distant observer (defined in eq. [5] and given numerically in this table by  $(M/R^3)^{1/2}$  in units where  $c = G = 1$ );  $\omega_s$ , angular velocity of the inertial frames at the *surface* of the star as measured by a distant observer (cf. eq. [4] and the subsequent discussion);  $\omega_c$ , angular velocity of the inertial frames at the *center* of the star, as measured by a distant observer;  $\delta R/R$ , fractional difference between the mean radius of the rotating star and the radius of the non-rotating star of the same central density (also equal to half the fractional difference in surface areas; cf. eq. [25]);  $\delta M/M$ , fractional difference in total mass-energies (cf. eq. [16]);  $\delta E_B/M_\odot$ , difference in binding energies (cf. eqs. [18] and [20]) in units of solar masses;  $e_s$ , eccentricity of the star's surface (cf. eq. [25c]);  $Q/(MR^2)$ , quadrupole moment of star (cf. eq. [26]) in units of  $MR^2$ .

TABLE 6  
SLOWLY ROTATING  $V_\gamma$  CONFIGURATIONS\*

$E_c, \text{ g/cm}^3$	$R_g/R$	$\Omega, \text{ sec}^{-1}$	$\omega_g/\Omega$	$\omega_c/\Omega$	$\delta R/R$	$\delta M/M$	$\delta E_B/M_\odot$	$e_g$	$Q/(MR^2)$
—	—	$\propto \Omega$	—	—	$\propto \Omega^2$	$\propto \Omega^2$	$\propto \Omega^2$	$\propto \Omega$	$\propto \Omega^2$
1.00E04	0.451	2.15E-2	1.0 E-6	5.9 E-6	0.194	0.313	1.86E-8	1.13	9.41E-2
1.00E05	.451	6.80E-2	4.7 E-6	3.4 E-5	.194	.314	2.87E-7	1.13	9.43E-2
1.00E06	.446	2.05E-1	1.92E-5	1.53E-4	.195	.303	3.27E-6	1.13	8.98E-2
1.00E07	.423	5.56E-1	5.45E-5	5.24E-4	.198	.259	1.77E-5	1.10	7.03E-2
1.00E08	.389	1.40E+0	1.09E-4	1.41E-3	.207	.202	4.62E-5	1.07	4.73E-2
1.00E09	.351	3.37E+0	1.75E-4	3.21E-3	.219	.152	7.42E-5	1.04	3.00E-2
1.00E10	.298	6.73E+0	1.82E-4	5.98E-3	.242	.0998	5.69E-5	1.02	1.55E-2
1.00E11	.242	1.36E+1	1.59E-4	1.05E-2	.266	.0587	3.05E-5	1.01	6.99E-3
1.00E12	.218	1.80E+1	1.41E-4	1.39E-2	.276	.0457	2.12E-5	1.01	4.84E-3
4.73E12	.214	1.16E+1	9.97E-5	1.56E-2	.280	.0482	1.75E-5	1.01	5.25E-3
1.00E13	.223	7.95E+0	8.48E-5	1.72E-2	.278	.0565	1.74E-5	1.01	6.56E-3
4.50E13	.293	2.68E+0	7.99E-5	2.34E-2	.252	.113	2.48E-5	1.03	1.72E-2
5.70E13	.314	1.72E+0	6.52E-5	2.50E-2	.246	.135	2.04E-5	1.03	2.23E-2
7.18E13	.297	5.38E-1	1.52E-5	2.66E-2	.264	.138	2.45E-6	1.03	2.20E-2
7.80E13	.0691	5.17E+0	1.77E-6	2.76E-2	.329	.00712	8.84E-8	1.00	7.55E-4
8.41E13	.0502	2.25E+1	2.45E-6	2.88E-2	.330	.00257	6.24E-8	1.00	2.29E-4
1.00E14	.0747	1.13E+2	1.63E-5	3.21E-2	.323	.00236	-6.18E-8	1.00	1.15E-4
2.40E14	.316	2.16E+3	3.32E-3	7.34E-2	.214	.0980	1.68E-4	1.02	1.33E-2
5.00E14	.500	6.46E+3	3.75E-2	2.12E-1	.154	.311	1.05E-2	1.11	8.98E-2
1.00E15	.589	1.03E+4	1.19E-1	4.46E-1	.111	.314	5.15E-2	1.11	1.08E-1
1.70E15	.637	1.33E+4	1.96E-1	6.28E-1	.0704	.256	5.73E-2	1.05	9.97E-2
3.00E15	.671	1.64E+4	2.63E-1	7.74E-1	.0308	.203	1.71E-2	0.986	9.64E-2
5.00E15	.682	1.88E+4	2.91E-1	8.57E-1	.0231	.172	-1.98E-2	0.946	9.34E-2
1.00E16	.676	2.11E+4	2.90E-1	9.20E-1	.0195	.149	-4.01E-2	0.920	8.54E-2
3.00E16	.649	2.21E+4	2.56E-1	9.58E-1	.0326	.137	-3.24E-2	0.917	7.19E-2
1.00E17	.622	2.15E+4	2.21E-1	9.79E-1	.0518	.142	-1.52E-2	0.933	6.33E-2
3.00E17	.614	2.06E+4	2.10E-1	9.89E-1	.0590	.149	-7.25E-3	0.942	6.21E-2
1.00E18	.620	2.03E+4	2.16E-1	9.94E-1	.0563	.153	-7.00E-3	0.944	6.49E-2
1.00E19	.626	2.06E+4	2.23E-1	9.99E-1	.0518	.150	-1.06E-2	0.939	6.62E-2
1.00E20	0.624	2.06E+4	2.21E-1	1.00E+0	0.0526	0.149	-1.08E-2	0.939	6.56E-2

\* For notation see footnote to Table 5.

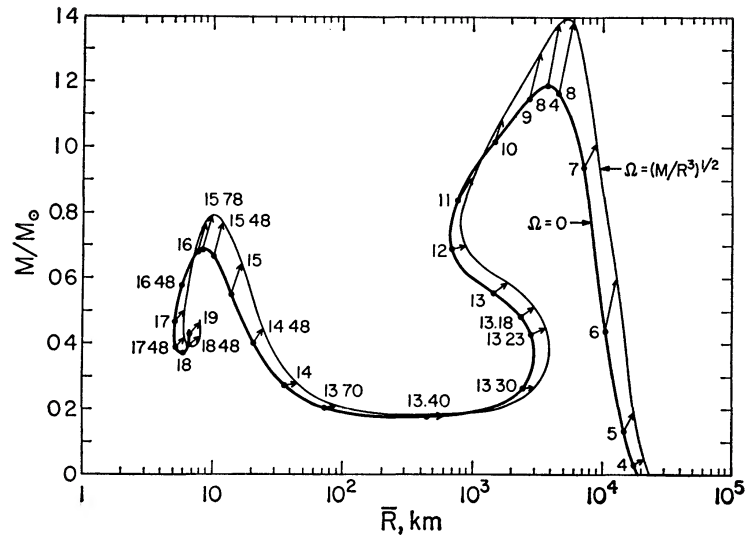


FIG. 1.—Effects of rotation on the masses and mean radii of HWW configurations. The thick curve is a plot of mass,  $M$ , versus radius,  $R$ , parameterized by the logarithm of central density in  $\text{g cm}^{-3}$ , for *non-rotating* HWW configurations. The thin curve is mass,  $M + \delta M$ , versus mean radius,  $\bar{R} = R + \delta R$ , for HWW configurations *rotating* with uniform angular velocity,  $\Omega = (M/R^3)^{1/2}$ . This angular velocity is approximately the amount needed to produce shedding of mass at the star's equator, so that our method of computation is not actually valid for this large a value of  $\Omega$ . For smaller angular velocities, where our method is valid, the deformation of the mass-radius curve is smaller by the dimensionless factor  $\Omega^2 R^3/M$ . The small arrows indicate the displacement, with increasing angular velocity, of configurations with the given central densities. To find the mass and mean radius of a configuration of given central density and given angular velocity, one moves out along the appropriate arrow by the fraction  $\Omega^2 R^3/M$  of the total length of the arrow.

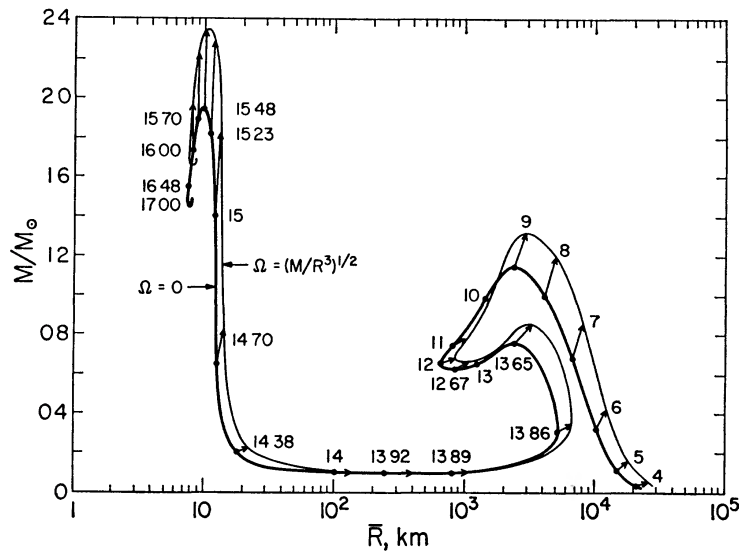


FIG. 2.—Effects of rotation on the masses and mean radii of  $V_\gamma$  configurations. The format of this figure is the same as that of Fig. 1.

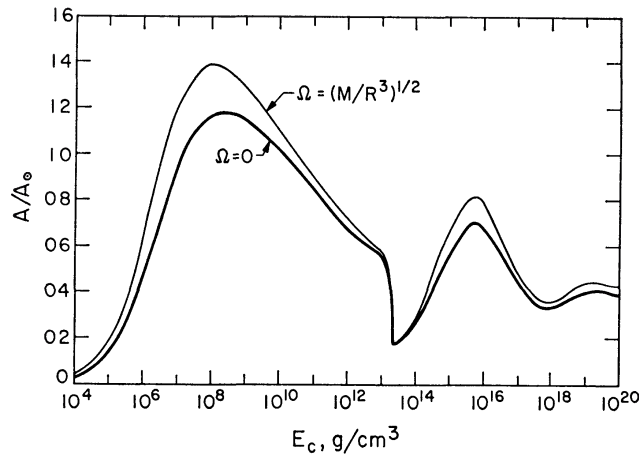


FIG. 3.—Effects of rotation on the number of baryons that HWW configurations contain. The number of baryons,  $A$ , in a configuration of given central density is plotted upward in units of the number of baryons in the Sun,  $A_{\odot} = 1.20 \times 10^{57}$ . The central density is plotted horizontally. The thick curve refers to non-rotating HWW configurations, and the thin curve refers to configurations with the “shedding” angular velocity,  $\Omega = (M/R^3)^{1/2}$ . For smaller angular velocities, the number of baryons is obtained by an upward displacement from the thick curve by the fraction  $\Omega^2 R^3/M$  of the distance to the thin curve.

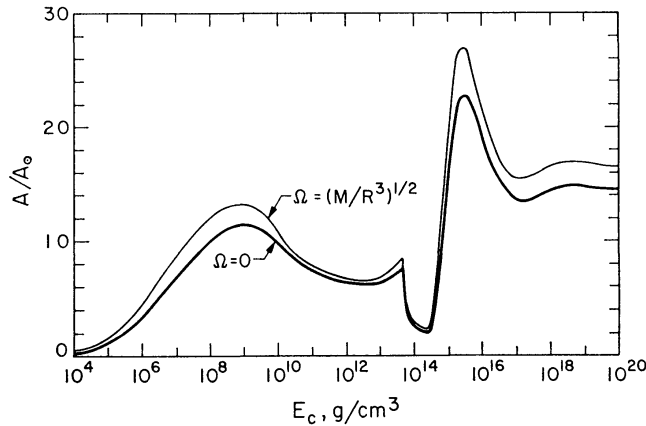


FIG. 4.—Effects of rotation on the number of baryons that  $V_{\gamma}$  configurations contain. The format of this figure is the same as that of Fig. 3.

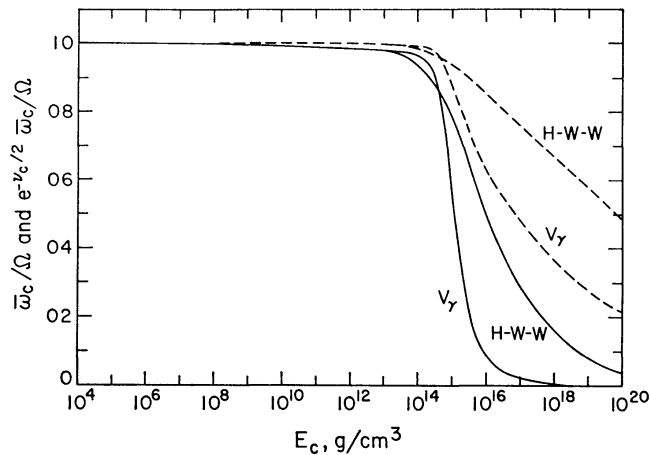


FIG. 5.—Dragging of inertial frames at the centers of HWW and  $V_{\gamma}$  configurations. Four curves are plotted—two for HWW configurations and two for  $V_{\gamma}$  configurations. The solid curves give  $\bar{\omega}_c/\Omega = (\Omega - \omega_c)/\Omega$ , which is the fluid angular velocity at the star’s center relative to the local inertial frames there, as measured by a distant observer, divided by the angular velocity of the fluid relative to the distant stars. The dashed curves give  $e^{-\nu c/2} \bar{\omega}_c/\Omega = e^{-\nu c/2} (\Omega - \omega_c)/\Omega$ , which is the same relative angular velocity, but this time as measured by an observer at the star’s center (time dilation factor  $e^{-\nu c/2}$  included).

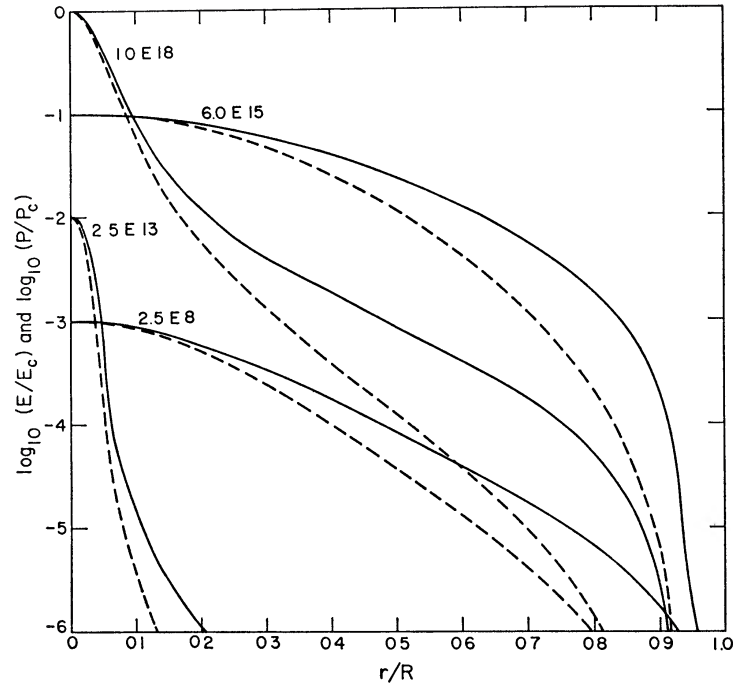


FIG. 6.—Distribution of energy density (*solid curves*) and pressure (*dashed curves*) inside four non-rotating HWW configurations. The logarithms of the energy density and pressure are plotted vertically, starting at an arbitrary point, which is different for each configuration. Coordinate radius is plotted horizontally in units of the total radius of the star. (Total radii,  $R$ , are given in Table 3.) The four configurations shown are the following: the most massive of the HWW white dwarfs, which has central density  $E_c = 2.5 \times 10^8 \text{ g cm}^{-3}$ ; the least massive HWW neutron star, with  $E_c = 2.5 \times 10^{13}$ ; the most massive HWW neutron star, with  $E_c = 6.0 \times 10^{15}$ ; and an unstable configuration of  $E_c = 1.0 \times 10^{18} \text{ g cm}^{-3}$ . The HWW white dwarfs, like the one shown here (*2.5 E8*), are all fairly homogeneous, as are the neutron stars of large mass ( $M \gtrsim 0.4 M_\odot$ ; e.g., curve *6.0 E15* here). The unstable stars and the neutron stars of low mass typically have small, dense, massive cores surrounded by diffuse, light envelopes (e.g., *2.5 E13* and *1.0 E18* shown here). For further discussion see Meltzer and Thorne (1966).

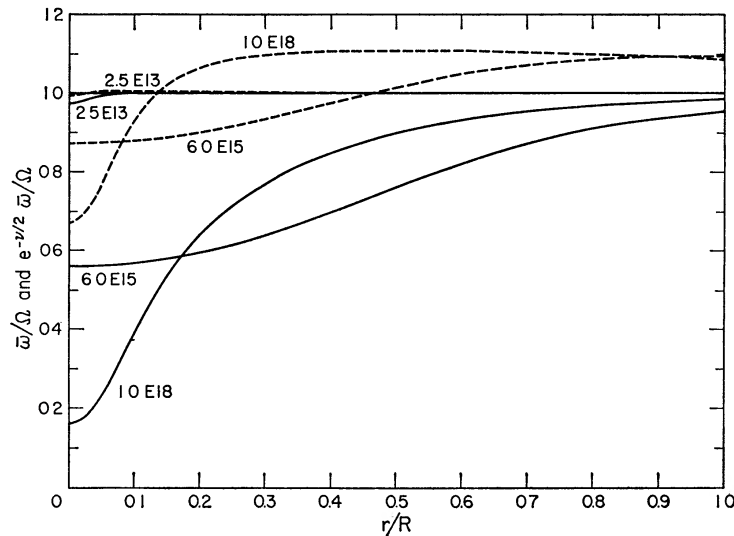


FIG. 7.—Dragging of inertial frames as a function of radius in four HWW configurations. The four configurations shown here are the ones whose density and pressure distributions are shown in Fig. 6; dragging of inertial frames is measured in terms of the same types of quantities as are used in Fig. 5. The solid curves give  $\bar{\omega}/\Omega = (\Omega - \omega)/\Omega$ , which is the fluid angular velocity at radius  $r$  relative to the local inertial frames there, as measured by a distant observer, divided by the angular velocity of the fluid with respect to the distant stars. The dashed curves give  $e^{-\nu/2} \bar{\omega}/\Omega = e^{-\nu/2} (\Omega - \omega)/\Omega$ , which is the same relative angular velocity, but this time as measured by an observer in the fluid at radius  $r$  (time dilation factor  $e^{-\nu/2}$  included).

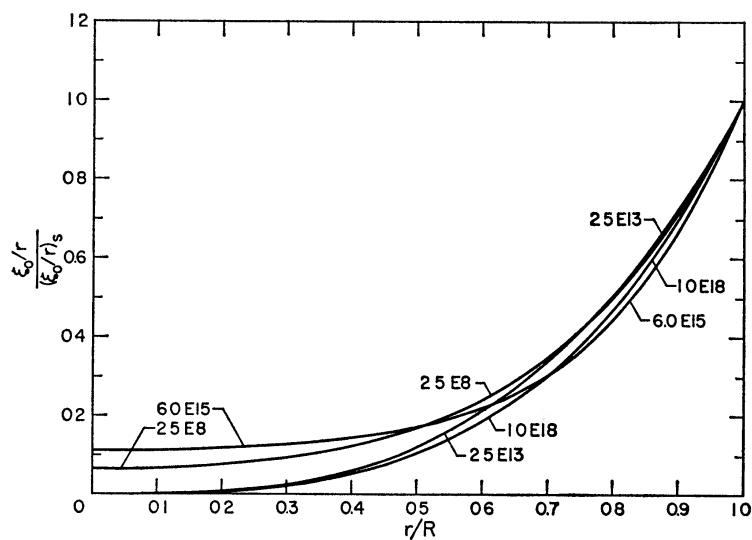


FIG. 8.—Spherical stretching due to rotation, as a function of radius in four HWW configurations. The four configurations shown here are the ones whose density and pressure distributions are shown in Fig. 6. The quantity plotted vertically is the fractional change in coordinate radius,  $\xi_0/r$ , of the surfaces of constant density at radius  $r$ , divided by the fractional change,  $(\xi_0/r)_s = \delta R/R$ , at the star's surface. In more invariant terms,  $\xi_0/r$  is one-half the fractional change in surface area of the surfaces of constant density (cf. eqs. [25]).

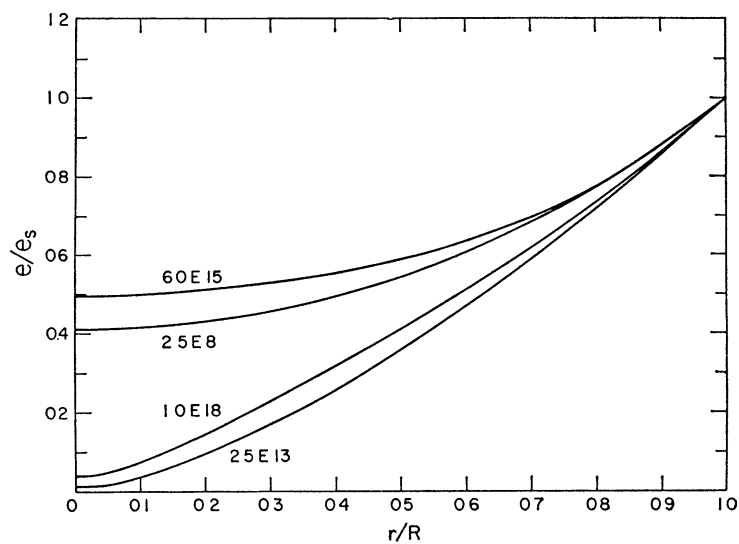


FIG. 9.—Rotational deformation as a function of radius in four HWW configurations. The four configurations shown here are the ones whose density and pressure distributions are shown in Fig. 6. The quantity plotted vertically is the eccentricity of the surfaces of constant density at radius  $r$ , divided by the eccentricity of the exterior surface of the star. (Recall that the intrinsic geometry of the surfaces of constant density is that of a spheroid; cf. eqs. [25].)

i) *Dragging of Inertial Frames*

The dragging of inertial frames as a function of radius is shown in Figure 7 for four representative HWW configurations and in Figure 11 for four representative  $V_\gamma$  configurations. The dragging of inertial frames as measured by a distant observer is always greatest at the star's center, and it decreases outward, verifying a theorem due to Hartle (1967). A comparison of Figure 7 with Figure 6, and Figure 11 with Figure 10, reveals information about the effect of the density distribution on the dragging of inertial frames: the more massive a given shell of matter, the greater the dragging on the inertial frames interior to it. In the white dwarfs and massive neutron stars, the density distribution is fairly homogeneous, so that the amount of dragging changes smoothly over the interior of

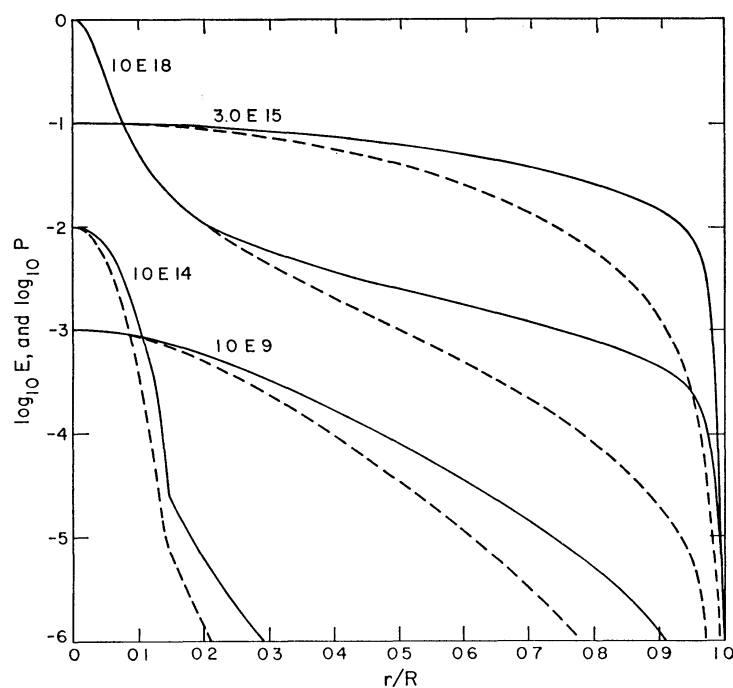


FIG 10.—Distribution of energy density (*solid curves*) and pressure (*dashed curves*) inside four non-rotating  $V_\gamma$  configurations. This figure is identical in format to Fig. 6. The density and pressure distributions are qualitatively similar to those for HWW configurations (cf. Fig. 6): white dwarfs and massive ( $M \gtrsim 0.4 M_\odot$ ) neutron stars have fairly homogeneous density and pressure distributions (Examples shown here: the most massive  $V_\gamma$  white dwarf, which has  $E_c = 1.0 \times 10^9 \text{ g cm}^{-3}$ ; and the most massive  $V_\gamma$  neutron star, which has  $E_c = 3.0 \times 10^{15}$ .) Unstable stars and neutron stars of low mass typically have small, dense, massive cores surrounded by diffuse, light envelopes. (Examples shown here: the least massive  $V_\gamma$  neutron star, which has  $E_c = 1.0 \times 10^{14}$ ; and the unstable configuration with  $E_c = 1.0 \times 10^{18}$ .)

the star. In the neutron stars of small mass and the unstable stars there is a high-density, high-mass core surrounded by a diffuse envelope. The dragging of frames in these stars peaks sharply in the core and is relatively small and slowly varying in the envelope.

The magnitude of the dragging of inertial frames shows a general increase with central density—i.e., an increase with increasing influence of relativity on the non-rotating stellar structure. This is evident in Figures 7 and 11; but it shows up much more vividly in Figure 5 and in Tables 5 and 6, where the values of the total dragging at the center and at the surface of a star are given as functions of central density. The dragging is negligible in white dwarfs ( $\lesssim 0.3$  per cent at the center;  $\lesssim 0.01$  per cent at the surface even when the star is near rotational shedding). However, the dragging is quite marked in neutron

stars (up to 25 per cent at the surface and 75 per cent at the center, as measured by a distant observer when the star is near rotational shedding). The dragging of frames is greater in  $V_\gamma$  neutron stars than in HWW neutron stars, because the  $V_\gamma$  neutron stars are more relativistic ( $2M/R$  is larger) and have more uniform density distributions. These properties of the  $V_\gamma$  neutron stars ultimately trace back to the fact that the  $V_\gamma$  equation of state is much stiffer near nuclear densities than the HW equation of state (see, e.g., Thorne 1967, chap. vii).

At any given radius the angular velocity of the fluid relative to the distant stars, or of the inertial frames relative to the distant stars, or of the fluid relative to the inertial frames, is greater when measured by a local observer than when measured by an observer far away, who looks down into the star. The difference in measurements is associated with the gravitational redshift of the photons by means of which the distant observer learns about the rotation. The angular velocities measured by the distant observer

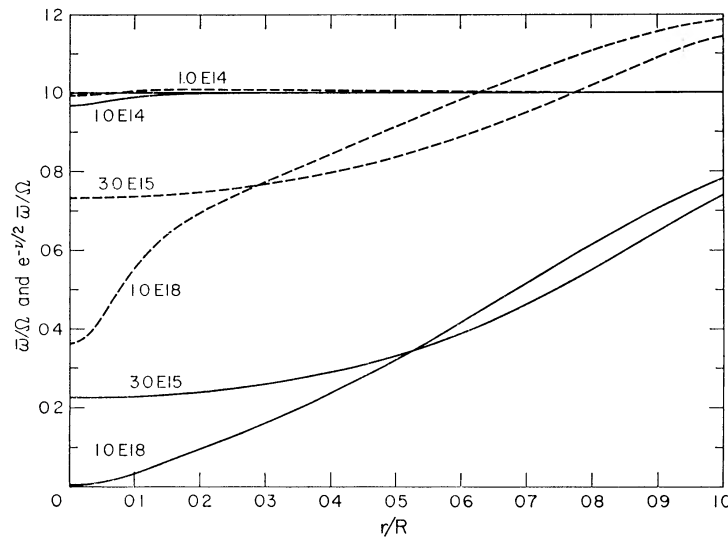


FIG. 11 —Dragging of inertial frames as a function of radius in four  $V_\gamma$  configurations. The four configurations here are the same as those in Fig. 10; the format of this figure is the same as that of Fig. 7.

are  $\Omega$ ,  $\omega$ , and  $\Omega - \omega = \bar{\omega}$ , and the angular velocities measured by a local observer are  $e^{-\nu/2}\Omega$ ,  $e^{-\nu/2}\omega$ , and  $e^{-\nu/2}\bar{\omega}$ . It is in terms of the observations of a distant observer that uniform angular velocity ( $\Omega = \text{constant}$ ) is defined. The effect of redshift on the angular velocities is exhibited in Figures 5, 7, and 11.

#### ii) Spherical Deformations: Change in Mass, Radius, and Baryon Number

In addition to producing quadrupole deformations (see next section), rotation produces a spherical stretching of a star and a consequent change in the mass, mean radius, and baryon content for fixed central density. The spherical stretching as a function of radius inside the star is shown graphically for four representative HWW configurations in Figure 8 and for four  $V_\gamma$  configurations in Figure 12. A comparison of Figure 8 with Figure 6, and Figure 12 with Figure 10, reveals information about the effect of the density distribution on the spherical stretching. In configurations with high-density cores and diffuse envelopes (HWW,  $E_c = 2.5 \text{ E13}$  and  $1.0 \text{ E18}$ ;  $V_\gamma$ ,  $E_c = 1.0 \text{ E14}$  and  $1.0 \text{ E18}$ ), the stretching is very small in the core and is sizable only in the outer parts of the envelope. When the density is more nearly homogeneous (HW,  $E_c = 2.5 \text{ E8}$  and  $6.0 \text{ E15}$ ;  $V_\gamma$ ,  $E_c = 1.0 \text{ E9}$ ; and, especially,  $V_\gamma$ ,  $E_c = 3.0 \text{ E15}$ ), the fractional spherical stretching

is more nearly uniform throughout the interior of the star. This general tendency is precisely what one expects on the basis of Newtonian intuition, as are the following aspects of the over-all magnitude of the stretching and of the changes in mass and baryon content.

The changes in mass, mean radius (i.e., surface area), and total baryon content due to rotation are given in Tables 5 and 6 and in Figures 1–4. Notice that the maximum masses and baryon numbers of neutron stars and of white dwarfs are increased by about 20 per cent as a result of uniform rotation near the mass-shedding angular velocity. For lower angular velocity, the increases in maximum mass and baryon number are proportionally smaller ( $\delta M$  and  $\delta A \propto \Omega^2$ ). Notice also that the masses, baryon numbers, and radii always increase for fixed central density as a result of rotation.

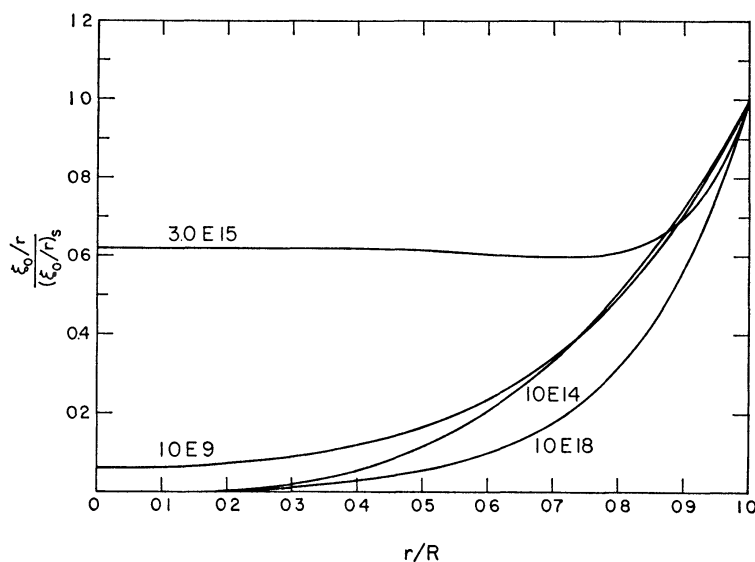


FIG. 12.—Spherical stretching due to rotation, as a function of radius in four  $V_\gamma$  configurations. The four configurations here are the same as those in Fig. 10; the format of this figure is the same as that of Fig. 8.

The fractional change in mean radius,  $\delta R/R$ , for  $\Omega^2 = M/R^3$  is fairly insensitive to central density,  $E_c$ , because for these angular velocities the ratio of centrifugal to gravitational force at the star's surface is fairly insensitive to  $E_c$ . The fractional changes in mass and baryon number,  $\delta M/M$  and  $\delta A/A$ , for  $\Omega^2 = M/R^3$  show large variations with central density. For configurations with dense cores and diffuse envelopes, the mass and baryon content are determined largely by the core, which is little affected by the rotation that produces mass shedding at the envelope's equator (cf. Figs. 8 and 12). Consequently, for core-envelope stars (unstable stars and small-mass neutron stars)  $\delta M/M$  and  $\delta A/A$  are small when  $\Omega^2 = M/R^3$ . For configurations with more uniform density distributions (white dwarfs and large-mass neutron stars), all regions of the star contribute significantly to the mass and baryon number, and the entire star is stretched (cf. Figs. 8 and 12); hence  $\delta M/M$  and  $\delta A/A$  are sizable.

The density distribution is also important in determining the radius of gyration (cf. Tables 5 and 6). Stars with dense cores and diffuse envelopes have small radii of gyration; stars with fairly uniform density distributions have large radii of gyration. Exceptions are the unstable stars of high central density. Because of the curvature of space inside these stars, their volumes are much larger than  $(4\pi/3)R^3$ . Consequently, when measured in units of  $R$ , their radii of gyration are much larger than Newtonian intuition

would suggest ( $R_g/R \sim 0.3\text{--}0.6$ , compared with  $R_g/R \ll 1$  as suggested by Newtonian intuition).

iii) *Quadrupole Deformations: Eccentricity and Quadrupole Moment*

The surfaces of constant density in a slowly rotating star have the intrinsic geometries of spheroids. The eccentricities of these spheroids (eq. [25c]) give a measure of the quadrupole deformation of the star. The eccentricity as a function of radius is shown graphically for our four representative HWW configurations in Figure 9 and for our four representative  $V_\gamma$  configurations in Figure 13. The quadrupole deformation has the same qualitative dependence on the density distribution as does the spherical stretching (cf. preceding section): for configurations with dense cores and diffuse envelopes the core is very little deformed compared with the envelope, whereas for configurations with more homogeneous density distributions the core and envelope deformations are comparable.

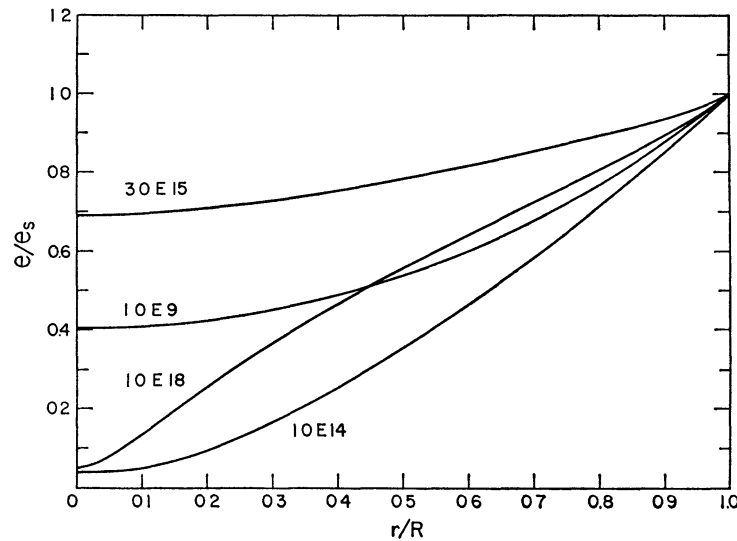


FIG. 13.—Rotational deformation as a function of radius in four  $V_\gamma$  configurations. The four configurations here are the same as those in Fig. 10; the format of this figure is the same as that of Fig. 9.

The eccentricities of the exterior surfaces of HWW and  $V_\gamma$  configurations are given in Tables 5 and 6 for  $\Omega^2 = M/R^3$ . Notice that the eccentricities are all very nearly unity. This is an indication that  $\Omega = (M/R^3)^{1/2}$  is, indeed, approximately the angular velocity for rotational shedding of mass—and also that our assumption of slow rotation is invalid for so large an angular velocity. For other angular velocities the eccentricity is smaller by the factor  $\Omega(R^3/M)^{1/2}$ .

In neutron stars the velocity of the surface when mass shedding occurs,

$$v_s = (M/R^3)^{1/2}R(1 - 2M/R)^{-1/2}, \quad (28)$$

is a significant fraction of the velocity of light (more than  $0.8c$  for the most massive neutron stars). By contrast, the surface velocity at mass shedding for white dwarfs is very small ( $\sim 10^{-2}c$  for the most massive). This difference is due to the fact that neutron stars are much more tightly bound than white dwarfs. In the sense that the slow-rotation approximation covers a greater range of surface velocities in neutron stars than in white dwarfs ( $\lesssim 0.1c$  compared to  $\lesssim 0.001c$ ), it is less restrictive for neutron stars than for white dwarfs. If measured, instead, by the ratio of rotational energy to gravitational potential energy for which slow rotation is valid, the slow-rotation approximation is equally restrictive in the two types of stars.

A measure of the deformation of the star's exterior gravitational field is its quadrupole moment,  $Q$  (see eq. [26] and the Appendix). The quadrupole moments of HWW and  $V_\gamma$  configurations are given in Tables 5 and 6 for  $\Omega^2 = M/R^3$ . The quadrupole moment has a behavior with central density similar to that of the radius of gyration: in units of  $M/R^3$  the quadrupole moment is largest for configurations of fairly uniform density and smallest for configurations with high-density cores and diffuse envelopes. For unstable configurations of very high central density, the quadrupole moments are larger than one might expect on Newtonian grounds, because the stellar volume is much larger than  $(4\pi/3)R^3$ .

#### iv) Stability

For non-rotating HWW and  $V_\gamma$  configurations, one can diagnose stability against radial perturbations from the form of the curve of mass versus radius (Figs. 1 and 2). (See, e.g., Thorne 1967, chap. iv.) One finds that only configurations below the first maximum of the curve (white dwarfs) and between the first minimum and second maximum (neutron stars) are stable.

For rotating configurations any definite statements about stability must await the completion of the dynamical-stability analysis, which is now in progress.

### IV. SUPERMASSIVE STARS

In contrast to neutron stars and white dwarfs, supermassive stars do not derive their pressure from the Fermi pressure of degenerate matter; rather, they rely upon large amounts of radiation pressure and small amounts of gas pressure. For masses  $M \gtrsim 10^3 M_\odot$ , stars can be approximated by relativistic polytropes of index 3. (See, e.g., Fowler 1966*b* and Thorne 1967 for reviews of the properties of supermassive stars.) The equation of state can then be put into the form

$$P = \mu N_c P^\dagger, \quad E = \mu N_c E^\dagger, \quad \epsilon = \mu N_c \epsilon^\dagger, \quad (29a)$$

$$\epsilon^\dagger = 3(1 - \beta/2)P^\dagger, \quad E^\dagger = (P^\dagger/a)^{3/4} + 3(1 - \beta/2)P^\dagger. \quad (29b)$$

Here  $\mu$  is the rest mass of a baryon,  $N_c$  is the central density of baryons,

$$a = P_c/\mu N_c \quad (29c)$$

is the ratio of central pressure to central density of rest mass, and

$$\beta \equiv \frac{P_{\text{gas}}}{(P_{\text{radiation}} + P_{\text{gas}})} \approx \frac{4.28}{(\text{mean molecular weight})} \times \frac{(\text{mass of Sun})^{1/2}}{(\text{mass of star})^{1/2}} \ll 1. \quad (29d)$$

The ratio  $\beta$  can be idealized as constant throughout the star. The quantities  $P^\dagger$ ,  $E^\dagger$ ,  $\epsilon^\dagger$  are dimensionless pressure, total energy density, and internal energy density, with the scale factor  $\mu N_c$  removed.

Bardeen (1965) points out that not only can the scale factor  $\mu N_c$  be removed from the equation of state (29) but it can also be removed from the equations of structure (3) for non-rotating stars by introduction of the dimensionless variables<sup>6</sup>

$$M^\dagger = M(\mu N_c)^{1/2}, \quad r^\dagger = r(\mu N_c)^{1/2}, \quad R^\dagger = R(\mu N_c)^{1/2}, \quad M_0^\dagger = \mu A(\mu N_c)^{1/2}. \quad (30)$$

<sup>6</sup> To remove the scale factor from eq. (3e), one must calculate rest mass,  $M_0 = \mu A$ , instead of  $A$ . The scale invariant form then becomes

The equations of structure for rotating stars (§ IIe, *f*, and *g* of this paper) exhibit the same scale invariance. If one computes the structure of a non-rotating or rotating supermassive star for given values of  $\alpha$  and  $\beta$  in terms of the dimensionless quantities  $M^\dagger$ ,  $m_0^\dagger$ ,  $m_2^\dagger$ ,  $r^\dagger$ ,  $E^\dagger$ , . . . , then one can scale his results to any desired value of the rest mass,  $M_0$ , by reintroducing the appropriate value of the scale factor,  $\mu N_c$ , and to any value of the angular velocity by performing the changes of scale discussed in § II.

The structures of non-rotating supermassive stars have been calculated by a number of people since Fowler and Hoyle first proposed that they might be formed in the nuclei of galaxies and that they might be the energy sources for quasi-stellar radio sources. (For reviews see Fowler 1966*b* and Thorne 1967.) The effects of general relativity on the structures of stable, non-rotating supermassive stars are negligible. General relativity does, however, play an important role in their stability: for any non-rotating star of mass greater than  $10^6 M_\odot$ , a relativistic instability causes gravitational collapse to begin before the star gets hot enough to burn its nuclear fuel. In order to avoid this instability, Fowler (1966*a*) turned his attention to the effects of rotation. Treating rotating stars by the post-Newtonian approximation to general relativity, Fowler found that rotation can stabilize stars of masses below  $10^8 M_\odot$  long enough for nuclear burning to occur; but for masses above  $10^8 M_\odot$ , the relativistic instability still dominates.

The question arose, however, as to whether *the full theory* of relativity will permit rotation to stabilize stars of  $M > 10^8 M_\odot$  long enough for nuclear burning to occur, even though the post-Newtonian approximation does not permit such stabilization. One way to attack this question, Fowler suggested (private communication), would be to calculate the binding energies of rotating, fully relativistic supermassive stars. If rotation can ever make the binding energies positive in the fully relativistic region—the region where stars of  $M > 10^8 M_\odot$  would burn hydrogen—then the corresponding stellar models might well be stable and be capable of living long enough to burn hydrogen. However, if the binding energies remain negative in the fully relativistic region for all reasonable angular velocities, then there is little hope of stabilization against collapse.

In order to carry out Fowler's suggestion, we have calculated the effects of uniform rotation on fully relativistic supermassive stars, using the method of dimensionless quantities outlined above. We concentrated our attention on models of rest mass  $M_0 > 10^6 M_\odot$ . For such models, the effects of the pressure parameter,  $\beta$ , are negligible whenever relativistic effects are appreciable. (To see this, one writes the binding energy—the only parameter significantly influenced by  $\beta$ —in the post-Newtonian approximation as

$$E_B/M_0 = E_B^\dagger/M_0^\dagger = [0.878\beta + 0.0442(\Omega^2 R^3/M)]\alpha - 6.94\alpha^2 \quad (31)$$

[cf. Fowler 1966*a*, *b*]. For  $M > 10^6 M_\odot$ , we have  $\beta < 10^{-2}$ ; hence, if  $\Omega^2 R^3/M \lesssim 1$  to avoid rotational shedding, and if  $\alpha > 10^{-2}$  [relativistic region], then the effect of  $\beta$  is negligible. We have also verified that  $\beta$  has negligible effect by calculating fully relativistic models with  $\beta \sim 10^{-2}$ – $10^{-4}$  and comparing them with models with  $\beta = 0$ .)

Because  $\beta$  has negligible effect in the relativistic region (region where  $\alpha > 10^{-2}$ ), we present here only stellar models with  $\beta = 0$ . In Table 7 we show the structures of the non-rotating stars, and in Table 8 we present the effects of rotation on the stellar structure. The binding energy and radius as functions of central density and of angular velocity are shown in Figure 14. Notice that rotation affects the radii considerably ( $\delta R/R \sim 0.3$  for

$$M_0^\dagger = \int_0^{R^\dagger} (E^\dagger - \epsilon^\dagger)(1 - 2M^\dagger/r^\dagger)^{-1/2} 4\pi r^{\dagger 2} dr^\dagger .$$

Note that the scale-invariant analysis of supermassive stars is possible only so long as  $\beta$  is taken to be a constant, i.e., only so long as  $\beta$  is not allowed to vary in accordance with eq (29d) when changes of scale are made.

TABLE 7  
NONROTATING SUPERMASSIVE STARS\*

$\alpha$	$E_c, \text{ g/cm}^3$	$M/M_0$	$E_B/M_0$	$R/2M^*$	$z_s$	$z_c$
1.00E-6	1.29E-15	1.000	-6.93E-12	4.30E5	1.16E-6	5.17E-6
3.00E-5	3.48E-11	1.000	-6.24E-09	1.45E4	3.46E-5	1.55E-4
1.00E-3	1.26E-06	1.000	-6.86E-06	4.39E2	1.14E-3	5.16E-3
1.00E-2	1.06E-03	1.001	-6.43E-04	4.83E1	1.05E-2	5.11E-2
3.00E-2	1.99E-02	1.005	-5.03E-03	2.00E1	2.60E-2	1.50E-1
1.00E-1	2.82E-01	1.037	-3.68E-02	1.19E1	4.51E-2	4.64E-1
1.40E-1	5.22E-01	1.059	-5.86E-02	1.23E1	4.31E-2	6.28E-1
2.10E-1	1.09E+00	1.093	-9.32E-02	1.70E1	3.07E-2	8.97E-1
2.60E-1	1.73E+00	1.110	-1.10E-01	2.51E1	2.05E-2	1.08E+0
3.00E-1	2.59E+00	1.116	-1.16E-01	3.82E1	1.34E-2	1.23E+0
3.50E-1	4.86E+00	1.111	-1.11E-01	6.46E1	7.83E-3	1.42E+0
4.00E-1	1.04E+01	1.095	-9.50E-02	9.02E1	5.59E-3	1.62E+0
4.50E-1	2.12E+01	1.081	-8.12E-02	8.52E1	5.92E-3	1.82E+0
4.90E-1	3.38E+01	1.074	-7.44E-02	7.54E1	6.70E-3	1.98E+0
5.30E-1	4.97E+01	1.070	-7.03E-02	6.43E1	7.87E-3	2.15E+0
6.80E-1	1.39E+02	1.066	-6.57E-02	4.41E1	1.15E-2	2.76E+0
8.00E-1	2.47E+02	1.067	-6.66E-02	3.78E1	1.35E-2	3.26E+0
1.00E+0	5.19E+02	1.070	-7.04E-02	3.41E1	1.50E-2	4.08E+0
1.40E+0	1.58E+03	1.077	-7.74E-02	3.44E1	1.48E-2	5.70E+0
1.70E+0	3.12E+03	1.080	-8.03E-02	3.60E1	1.42E-2	6.91E+0
2.10E+0	6.89E+03	1.081	-8.12E-02	3.97E1	1.28E-2	8.52E+0
3.00E+0	2.87E+04	1.079	-7.93E-02	4.17E1	1.22E-2	1.22E+1

\* Supermassive stars are here idealized as polytropes of index 3 with  $\beta = P_{\text{gas}}/P_{\text{total}} = 0$ . The various columns are:  $\alpha$ , ratio of central pressure to central density of rest mass;  $E_c$ , central density of total mass-energy for the special case of rest mass  $M_0 = \mu A = 10^8 M_\odot$ ;  $M/M_0$ , total mass-energy of star in units of rest mass;  $E_B/M_0$ , binding energy of star in units of rest mass;  $R/2M^*$ , radius of star in units of its gravitational radius,  $2M^* = 2GM/c^2$ ;  $z_s$ , gravitational redshift,  $\Delta\lambda/\lambda$ , of a photon emitted from the star's surface and received at infinity;  $z_c$ , gravitational redshift of a neutrino emitted from the star's center and received at infinity. This table is valid to accuracy 1 per cent or better for the more realistic models with  $\beta$  given by equation (29d), with one exception: For small  $\alpha$  ( $\alpha < 10^{-2}$ ) the binding energy must be replaced by

$$E_B/M_0 = 0.878\beta\alpha - 6.94\alpha^2.$$

TABLE 8  
SLOWLY ROTATING SUPERMASSIVE STARS\*

$\alpha$	$R_g/R$	$\Omega, \text{sec}^{-1}$	$\omega_g/\Omega$	$\omega_c/\Omega$	$\delta R/R$	$\delta M/M$	$\delta E_B/M_\odot$	$e_g$	$Q/(MR^2)$
—	—	$\propto \Omega$	—	—	$\propto \Omega^2$	$\propto \Omega^2$	$\propto \Omega^2$	$\propto \Omega$	$\propto \Omega^2$
1.00E-6	0.273	2.56E-12	1.71E-7	5.35E-6	0.246	7.41E-2	4.33E-8	1.014	9.36E-3
3.00E-5	.271	4.14E-10	5.07E-6	2.05E-4	.247	7.22E-2	1.26E-6	1.013	8.96E-3
1.00E-3	.270	7.81E-08	1.65E-4	6.84E-3	.247	7.09E-2	4.07E-5	1.013	8.71E-3
1.00E-2	.267	2.14E-06	1.48E-3	6.41E-2	.248	6.53E-2	3.21E-4	1.010	7.69E-3
3.00E-2	.256	8.02E-06	3.29E-3	1.69E-1	.252	5.24E-2	5.45E-4	1.005	5.53E-3
1.00E-1	.212	1.70E-05	3.80E-3	3.94E-1	.273	2.73E-2	2.61E-4	1.000	2.17E-3
1.40E-1	.185	1.56E-05	2.78E-3	4.71E-1	.286	1.97E-2	1.34E-4	1.000	1.39E-3
2.10E-1	.139	9.35E-06	1.13E-3	5.66E-1	.305	1.13E-2	6.58E-5	1.000	6.95E-4
2.60E-1	.112	5.15E-06	4.99E-4	6.15E-1	.315	8.39E-3	5.09E-5	1.000	4.95E-4
3.00E-1	.0962	2.74E-06	2.42E-4	6.47E-1	.319	6.93E-3	3.69E-5	1.000	3.95E-4
3.50E-1	.0922	1.25E-06	1.32E-4	6.82E-1	.321	7.33E-3	2.71E-5	1.001	4.40E-4
4.00E-1	.0977	7.67E-07	1.06E-4	7.12E-1	.319	8.44E-3	2.39E-5	1.001	4.97E-4
4.50E-1	.112	8.47E-07	1.48E-4	7.39E-1	.315	1.14E-2	3.33E-5	1.001	7.14E-4
4.90E-1	.119	1.02E-06	1.88E-4	7.57E-1	.313	1.25E-2	4.14E-5	1.001	7.78E-4
5.30E-1	.128	1.30E-06	2.53E-4	7.73E-1	.310	1.44E-2	5.42E-5	1.001	9.41E-4
6.80E-1	.139	2.30E-06	4.37E-4	8.20E-1	.306	1.62E-2	8.41E-5	1.001	1.07E-3
8.00E-1	.141	2.90E-06	5.22E-4	8.46E-1	.305	1.61E-2	9.41E-5	1.001	1.06E-3
1.00E+0	.138	3.38E-06	5.58E-4	8.77E-1	.306	1.50E-2	9.42E-5	1.001	9.61E-4
1.40E+0	.130	3.30E-06	4.89E-4	9.14E-1	.309	1.31E-2	8.09E-5	1.001	8.17E-4
1.70E+0	.128	3.08E-06	4.56E-4	9.30E-1	.310	1.32E-2	7.74E-5	1.001	8.47E-4
2.10E+0	.123	2.66E-06	3.81E-4	9.45E-1	.311	1.21E-2	6.73E-5	1.001	7.48E-4
3.00E+0	0.126	2.48E-06	3.79E-4	9.64E-1	0.311	1.31E-2	6.93E-5	1.001	8.37E-4

\* Supermassive stars are here idealized as polytropes of index 3 with  $\beta = P_{\text{gas}}/P_{\text{total}} = 0$ . This table is valid to accuracy 1 per cent or better for the more realistic models with  $\beta$  given by equation (29d), with one exception: For small  $\alpha$  ( $\alpha < 10^{-2}$ ) the binding energy must be replaced by equation (31). The notation is the same as that of Table 5 with two exceptions: The column labeled " $\Omega, \text{sec}^{-1}$ " gives the angular velocity  $\Omega = (M/R^3)^{1/2}$  for the special case of a star with rest mass  $M_0 = 10^8 M_\odot$ ; and the change in binding energy,  $\delta E_B$ , is measured in units of the star's rest mass instead of in solar masses.

$\Omega^2 = M/R^3$ ) but has very little effect on the binding energies ( $\delta E_B/E_B \sim -10^{-3}$  for  $\Omega^2 = M/R^3$ ). Consequently, *it appears highly unlikely that uniform rotation can stabilize stars of  $M > 10^5 M_\odot$  in the relativistic region  $\alpha > 10^{-2}$ .* We are now studying the effects of rotation on stability in order to verify this conjecture.

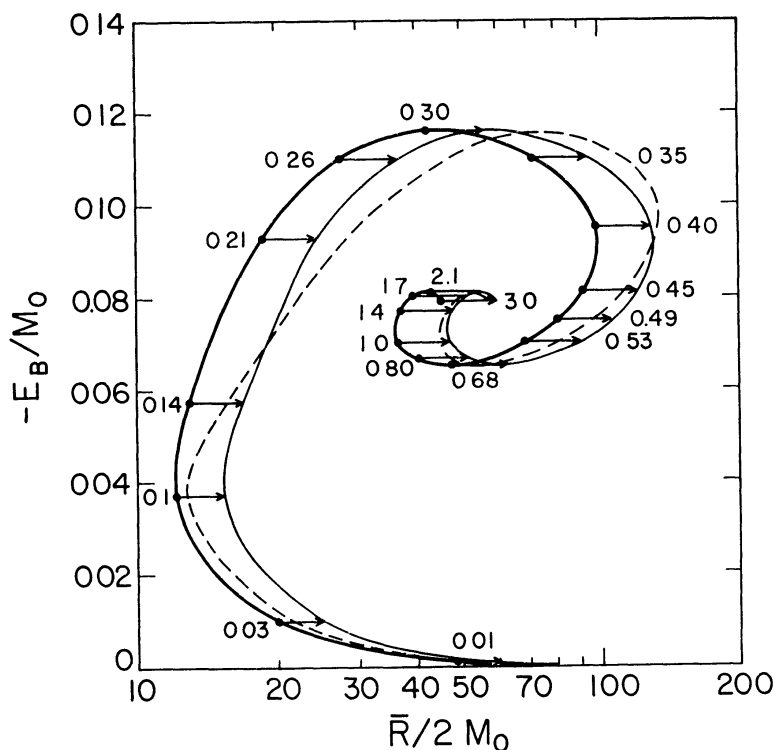


FIG. 14.—Effects of rotation on the binding energies and mean radii of supermassive stars. The supermassive stars are here idealized as relativistic polytropes of index 3 with  $\beta = P_{\text{gas}}/P_{\text{total}} \ll 1$ .  $\beta$  has negligible effect on the curves of this figure if the stars have rest mass  $M_0 > 10^5 M_\odot$ . Hence these curves were calculated for  $\beta = 0$ . The thick curve is a plot of the negative of the fractional binding energy,  $-E_B/M_0$ , versus radius,  $R$ , measured in units  $2M_0 \approx$  (gravitational radius). The curve is parameterized by  $\alpha$ , the ratio of pressure to density of rest mass at the center of the star. The thin solid curve is fractional binding energy,  $(E_B + \delta E_B)/M_0$ , versus mean radius,  $\bar{R} = R + \delta R$ , for rotating configurations with angular velocity  $\Omega = (M/R^3)^{1/2}$ . To find the binding energy and mean radius for other angular velocities, one moves out along the arrow corresponding to the desired value of  $\alpha$  by the fraction  $\Omega^2 R^3/M$  of the total length of the arrow. Also shown on this figure is binding energy versus mean radius for configurations of fixed angular momentum,  $J = 0.16 M_0^2$  (dashed curve). It is along such a curve that a star of fixed rest mass would try to evolve if it were stable—which these stars are probably not—and if it were not shedding mass at its equator. The curves shown here are valid only for  $\alpha \gtrsim 0.01$ . For smaller values of  $\alpha$ , the post-Newtonian formula (31) is valid.

We are indebted to William A. Fowler for helpful discussions of supermassive stars, to Barbara A. Zimmerman for assistance with the numerical calculations, and to B. Kent Harrison, Sachiko Tsuruta, and A. G. W. Cameron for permission to present Tables 1 and 2 of the HW and  $V_\gamma$  equations of state. Part of this work was performed while the authors were participating in the summer 1967 International Research Group in Relativistic Astrophysics at the Institut d'Astrophysique in Paris. We thank the Institut d'Astrophysique and Professor Evry Schatzman for their kind hospitality.

## APPENDIX

## THE EXTERIOR GRAVITATIONAL FIELD

From equations (4), (11), (15c), (17a), (22), and (23), one obtains as the external gravitational field of the rotating star, accurate to second order in the angular velocity,

$$\begin{aligned}
 ds^2 = & -\left(1 - 2\frac{\mathfrak{M}}{r} + 2\frac{J^2}{r^4}\right)\left\{1 + 2\left[\frac{J^2}{\mathfrak{M}r^3}\left(1 + \frac{\mathfrak{M}}{r}\right) \right. \right. \\
 & \left. \left. + \frac{5}{8}\frac{Q - J^2/\mathfrak{M}}{\mathfrak{M}^3}Q_2^2\left(\frac{r}{\mathfrak{M}} - 1\right)\right]P_2(\cos\theta)\right\}dt^2 \\
 & + \left(1 - 2\frac{\mathfrak{M}}{r} + 2\frac{J^2}{r^4}\right)^{-1}\left\{1 - 2\left[\frac{J^2}{\mathfrak{M}r^3}\left(1 - \frac{5\mathfrak{M}}{r}\right) \right. \right. \\
 & \left. \left. + \frac{5}{8}\frac{Q - J^2/\mathfrak{M}}{\mathfrak{M}^3}Q_2^2\left(\frac{r}{\mathfrak{M}} - 1\right)\right]P_2(\cos\theta)\right\}dr^2 \quad (\text{A1}) \\
 & + r^2\left[\left[1 + 2\left\langle -\frac{J^2}{\mathfrak{M}r^3}\left(1 + \frac{2\mathfrak{M}}{r}\right) + \frac{5}{8}\frac{Q - J^2/\mathfrak{M}}{\mathfrak{M}^3}\left\{\frac{2\mathfrak{M}}{[r(r - 2\mathfrak{M})]^{1/2}} \right. \right. \right. \right. \right. \\
 & \left. \left. \left. \left. \times Q_2^1\left(\frac{r}{\mathfrak{M}} - 1\right) - Q_2^2\left(\frac{r}{\mathfrak{M}} - 1\right)\right\}\right\rangle P_2(\cos\theta)\right]\right] \\
 & \times \left\{d\theta^2 + \sin^2\theta\left[d\phi - \left(\frac{2J}{r^3}\right)dt\right]^2\right\}.
 \end{aligned}$$

The only constants that enter into this line element are the total mass of the rotating star,  $M + \delta M \equiv \mathfrak{M}$ ; the star's total angular momentum,  $J$ ; and the star's mass quadrupole moment,  $Q$ . (Whenever  $M$  appears in a term of second order in  $\Omega^2$ , it can be replaced by  $\mathfrak{M}$  without affecting the line element to order  $\Omega^2$ .)

The three parameters  $\mathfrak{M}$ ,  $J$ , and  $Q$ , which characterize the exterior metric of a slowly rotating object, are invariantly defined. This is well known in the case of the mass and the angular momentum (see, e.g., Papapetrou 1948; Hartle and Sharp 1967).

An invariant definition of the quadrupole moment can be given as follows: For a static metric there is a unique timelike Killing vector whose length can be normalized to 1 at infinity. In our coordinate system,  $\xi^\mu = \delta_t^\mu$ . The length of the vector,  $\sigma^2 = -\xi^\alpha\xi_\alpha$ , is an invariant; and in our coordinate system,  $\sigma = (-g_{tt})^{1/2}$ . Consider the surfaces of constant  $\sigma$ . These invariantly defined surfaces can be described by embedding them in a three-dimensional space exactly as was done for the surfaces of constant density in § II. The embedded surfaces have the geometry of spheroids with eccentricities, which, at large distances  $r^*$  from the origin, behave like

$$e = \left(\frac{3Q}{Mr^{*2}}\right)^{1/2} + O\left(\frac{1}{r^{*2}}\right). \quad (\text{A2})$$

The quadrupole moment can thus be defined invariantly in terms of the leading coefficient in the asymptotic behavior of the eccentricity,  $e$ , which describes the distortion of the intrinsic geometry of the surfaces of constant timelike Killing-vector length.

For stars, such as the Sun, which are not very relativistic (i.e.,  $\mathfrak{M}/r \ll 1$ ), the line element (A1) can be expanded in powers of  $\mathfrak{M}/r$ . For the Sun, the relative magnitudes of the various quantities in the external line element are

$$\mathfrak{M}/r < \mathfrak{M}/R \approx 2 \times 10^{-6}, \quad J/r^2 < J/R^2 \sim 10^{-12}, \quad Q/r^3 < Q/R^3 \lesssim 10^{-10}. \quad (\text{A3})$$

Consequently, to an accuracy of the order of 1 part in  $10^{15}$ , the external line element for the Sun is

$$ds^2 = - \left[ 1 - \frac{2\mathcal{M}}{r} + \frac{2Q}{r^3} P_2(\cos \theta) \right] dt^2 + \left[ 1 - \frac{2\mathcal{M}}{r} + \frac{2Q}{r^3} P_2(\cos \theta) \right]^{-1} dr^2 \\ + \left[ 1 - \frac{2Q}{r^3} P_2(\cos \theta) \right] r^2 \left\{ d\theta^2 + \sin^2 \theta \left[ d\phi - \frac{2J}{r^3} dt \right]^2 \right\}. \quad (\text{A4})$$

The terms in  $2\mathcal{M}/r$  account for the Newtonian gravitational attraction and the relativistic perihelion shift of Mercury's orbit, and the terms in  $2Q/r^3$  produce a perihelion shift associated with the Sun's oblateness (Dicke and Goldenberg 1967). The term in  $2J/r^3$  produces a dragging of inertial frames that also leads to a precession of Mercury's perihelion with respect to the distant stars, but a precession that is negligibly small in the case of the Sun. From the line element (A4), one can readily verify that the perihelion shift of Mercury due to a slightly oblate, rotating Sun is very accurately given by adding the relativistic shift for the spherical Sun to the oblateness shift for the deformed Newtonian Sun.

The line element given in equation (A1) describes correctly the geometry outside *any* slowly rotating configuration. It is interesting to compare it with the only known exact solution exterior to a rotating object—the Kerr metric (Kerr 1963). To second order in the angular velocity, the Kerr metric given in the form of Boyer and Lindquist (1967, eq. [2.13]) can be transformed to the form of equation (A1) by the transformation

$$r \rightarrow r \left\{ 1 - \frac{a^2}{2r^2} \left[ \left( 1 + \frac{2\mathcal{M}}{r} \right) \left( 1 - \frac{\mathcal{M}}{r} \right) + \cos^2 \theta \left( 1 - \frac{2\mathcal{M}}{r} \right) \left( 1 + \frac{3\mathcal{M}}{r} \right) \right] \right\}, \quad (\text{A5}) \\ \theta \rightarrow \theta - a^2 \cos \theta \sin \theta \frac{1}{2r^2} \left( 1 + \frac{2\mathcal{M}}{r} \right).$$

It is then seen easily that, for the Kerr solution,  $J = -\mathcal{M}a$  and  $Q = J^2/\mathcal{M}$ . These results are the same as those derived by Hernandez (1967) by a different method. The special relationship  $Q = J^2/\mathcal{M}$  between the quadrupole moment and the angular momentum shows the very special nature of the Kerr solution.

#### REFERENCES

- Bardeen, J. M. 1965, unpublished Ph.D. thesis; available from University Microfilms, Inc., Ann Arbor, Michigan.
- Boyer, R. H., and Lindquist, R. W. 1967, *J. Math. Phys.*, **8**, 265.
- Dicke, R. H., and Goldenberg, H. M. 1967, *Phys. Rev. Letters*, **18**, 313.
- Fowler, W. A. 1966a, *Ap. J.*, **144**, 180.
- . 1966b, in *High-Energy Astrophysics* (Proc. Course 35, Internat. School of Physics Enrico Fermi), ed. L. Gratton (New York: Academic Press).
- Harrison, B. K., Thorne, K. S., Wakano, M., and Wheeler, J. A. 1965, *Gravitation Theory and Gravitational Collapse* (Chicago: University of Chicago Press).
- Harrison, B. K., Wakano, M., and Wheeler, J. A. 1958, in *La Structure et l'évolution de l'univers* (Onzième Conseil de Physique Solvay) (Brussels: Stoops).
- Hartle, J. B. 1967, *Ap. J.*, **150**, 1005 (Paper I).
- Hartle, J. B., and Sharp, D. H. 1967, *Ap. J.*, **147**, 317.
- Hernandez, W. C., Jr. 1967, *Phys. Rev.*, **159**, 1070.
- Kerr, R. 1963, *Phys. Rev. Letters*, **11**, 552.
- Landau, L., and Lifshitz, E. M. 1962, *Classical Theory of Fields* (Reading, Mass.: Addison-Wesley Publishing Co.).
- Meltzer, D. W., and Thorne, K. S. 1966, *Ap. J.*, **145**, 514.
- Oppenheimer, J. R., and Volkoff, G. M. 1939, *Phys. Rev.*, **55**, 374.
- Papapetrou, A. 1948, *Proc. Roy. Irish Acad.*, **52**, 11.
- Thorne, K. S. 1967, in *Hautes énergies en astrophysique*, Vol. 3, ed. C. DeWitt, E. Schatzman, and P. Véron (New York: Gordon & Breach).
- Tsuruta, S., and Cameron, A. G. W. 1966, *Canadian J. Phys.*, **44**, 1895.
- Wheeler, J. A. 1967, *Ann. Rev. Astr. and Ap.*, **4**, 393.